Supporting Information

Tunable Optical and thermodynamic characters: The ignition ways of energetic metal complexes with different crystal fields

Kun Wang [a, b*], Xiaoqi Yang [a], Peipei Zhang [a], Shu Bu [a], Longjiu Cheng [a], Jianguo Zhang[b]

[a] *Department of Chemistry, Key Laboratory of Functional Inorganic Materials of Anhui Province, Anhui University, Hefei, Anhui 230601, P. R. China*

[b]*State Key Laboratory of Explosion Science and Technology, Beijing Institute of Technology, Beijing 100081 P. R. China*

*Corresponding Author: Kun Wang: wangkun@ahu.edu.cn

Contents

Section 1 The confirmation of theoretical methods

The cut-off energy test (with the cutoff energy of 900eV) and k-point test (with the k-points grid of 2×2×4 Monkhorst-Pack meshes of Cr, Fe, Co, Ni, Cu, Zn, and 2×2×2 Monkhorst Pack meshes of Mn) are summarized in Table S1~S2. Based on the tests, we have confirmed the k-points of 2×2×4 and cutoff energy of 900 eV for Cr, Fe, Co, Ni, Cu, Zn, and 2×2×2 and cutoff energy of 900 eV for Mn in the optimization. The convergence standards we applied in the optimization is maintained as: 1) the energy is less than 1×10^{-5} eV/atom; 2) max force is less than 0.03 eV/Å; 3) max stress is less than 0.05 GPa and 4) the displacement is less than 0.001 Å .

Table S1 The tests of k-point grids and cutoff energy of $[Zn(DAT)_6(ClO_4)_2$.

$[Zn(DAT)_6(ClO_4)_2$		
K points (Monkhorst-pack grid)	Energy (eV)	Time (s)
1×1×1	-17071.531	134.43
1×1×2	-17077.268	176.19
2×1×2	-17071.944	402.98
2×2×2	-17071.938	318.84
2×2×3	-17077.247	401.17
2×2×4	**-17077.246**	**615.07**
2×4×2	-17077.250	791.55
3×1×2	-17071.944	827.69
Cutoff energy	Energy (eV)	Time (s)
600	-17070.937	477.49
700	-17071.291	643.80
750	-17071.486	539.14
800	-17071.663	702.23
850	-17071.815	905.13
900	**-17077.246**	**615.07**

Table S2 The tests of k-point grids and cutoff energy of $[Mn(DAT)_6(ClO_4)_2$.

$[Mn(DAT)_6(ClO_4)_2$		
K points (Monkhorst-pack grid)	Energy (eV)	Time (s)
1×1×1	-32031.913	1231.61
1×1×2	-32031.912	1581.46
1×2×1	-32031.904	1074.10
2×1×1	-32031.904	1236.01
2×1×2	-32031.904	954.88
2×2×1	-32031.894	1325.56
2×2×2	**-32031.895**	**1325.56**
2×2×3	-32031.895	10374.58
2×4×2	-32031.895	2876.33
3×1×2	-32031.895	3122.89
Cutoff energy	Energy (eV)	Time (s)
700	-32030.621	746.32
750	-32031.009	1044.95
800	-32031.367	663.14
850	-32031.659	1002.61
900	**-32031.895**	**1445.20**
950	-32032.075	1933.24
1000	-32032.200	1602.70

Section 2 Gas-phase structural parameters

We have done the benchmark DFT calculation with different basis sets and corresponding time cost for gas-phase $[Zn(DAT)_6](ClO_4)_2$.

Table S3 The benchmark calculation of the gas-phase structure of $[Zn(DAT)_6](ClO_4)_2$.

	Typical bond length and angles	time
	Zn-N1/N1-CI/N1-N2/N2-N3/N3-N4/N4-C1/N4-N5/N6-C1	
Experimental results	2.218/1.332/1.373/1.274/1.355/1.339/1.386/1.317	
6-311G**/m062x	2.225/1.329/1.350/1.267/1.353/1.349/1.378/1.335	18h32m
M062X/def2svp	2.283/1.334/1.340/1.266/1.345/1.353/1.368/1.328	4h28m
M062X/def2tzvp	2.359/1.328/1.349/1.264/1.347/1.347/1.375/1.332	2d19h8m
B3LYP/def2tzvp	2.421/1.335/1.356/1.273/1.358/1.356/1.379/1.328	1d1h28m
TPSSh/def2tzvp	2.354/1.338/1.358/1.277/1.360/1.357/1.383/1.328	1d3h4m
BPW91/def2tzvp	2.407/1.346/1.363/1.287/1.369/1.367/1.384/1.330	21h29m
M062X/def2qzvp	2.320/1.329/1.349/1.264/1.346/1.347/1.375/1.331	18d16h51m

Table S4 The nature population analysis (NPA) charges of metals and coordinated atoms, bond distances (D(Å)) and Wiberg bond index(WBI (a.u)) of coordinative bonds, configuration of center metal for **(a)** **[**$Cr(DAT)_6](ClO_4)_2$; **(b)** **[**$Mn(DAT)_6](ClO_4)_2$; **(c)** **[**$Fe(DAT)_6](ClO_4)_2$; **(d)[**$Co(DAT)_6](ClO_4)_2$; **(e)** **[**$Ni(DAT)_6](ClO_4)_2$; **(f)** **[**$Cu(DAT)_6](ClO_4)_2$; **(g)** **[**$Zn(DAT)_6](ClO_4)_2$.

Molecule	**NPA change (e)**	**M-N1/M-N1a/ M-N1b/M-N1c/ M-N1d/M-N1e**		**N1-N2/N2-N3/N3-N4/ N4-C1/C1-N6/N4-N5/Cl-O**	**configuration**	**ΔE** (kcal/mol)
	N1/N1a/N1b/N1c /M/N1d/N1e	D (Å)	WBI (a.u.)	D (Å)		
(a)	-0.47/-0.53/-0.54/-0.49 /1.61/-0.56/-0.52	2.53/2.15/ 2.16/2.39/ 2.14/2.17	0.05/0.05/0.15/ 0.06/0.06/0.14	1.39/1.29/1.38/ 1.36/1.33/1.37/1.73	$(t2g)^4(eg)^0$	36.03
(b)	-0.51/-0.52/-0.55/-0.56 /1.72/-0.55/-0.54	2.29/2.30/ 2.26/2.21/ 2.22/2.22	0.07/0.07/0.08/ 0.08/0.08/0.08	1.39/1.29/1.39/ 1.36/1.33/1.37/1.74	$(t2g)^5(eg)^0$	68.80
(c)	-0.50/-0.54/-0.53/-0.56 /1.71/-0.56/-0.53	2.29/2.21/ 2.22/2.18/ 2.20/2.20	0.07/0.08/0.08/ 0.08/0.09/0.09	1.39/1.29/1.38/ 1.36/1.33/1.37/1.72	$(t2g)^5(eg)^1$	50.51
(d)	-0.49/-0.55/-0.53/-0.54 /1.69/-0.53/-0.54	2.26/2.17/ 2.23/2.13/ 2.27/2.14	0.08/0.09/0.08/ 0.09/0.09/0.10	1.38/1.29/1.38/ 1.36/1.33/1.37/1.73	$(t2g)^5(eg)^2$	33.55
(e)	-0.51/-0.51/-0.53/-0.55 /1.66/-0.54/-0.53	2.17/2.20/ 2.17/2.11/ 2.12/2.11	0.08/0.08/0.13/ 0.18/0.05/0.06	1.39/1.29/1.39/ 1.36/1.33/1.37/1.73	$(t2g)^6(eg)^2$	
(f)	-0.47/-0.55/-0.55/-0.56 /1.66/-0.58/-0.53	2.54/2.07/ 2.08/2.31/ 2.05/2.09	0.05/0.10/0.11/ 0.05/0.11/0.11	1.39/1.29/1.38/ 1.36/1.33/1.37/1.73	$(t2g)^6(eg)^3$	
(g)	-0.50/-0.55/-0.55/-0.57 /1.75/-0.56/-0.54	2.28/2.17/ 2.17/2.14/	0.07/0.07/0.08/ 0.07/0.08/0.08	1.39/1.29/1.38/ 1.36/1.33/1.37/1.73	$(t2g)^6(eg)^4$	

Section 3 Calculation of Crystal structures

3.1 Theoretical cell parameters of crystal structures

In the optimization, the convergence standards we applied is maintained as: 1) the energy is less than 1×10^{-5} eV/atom; 2) max force is less than 0.03 eV/Å; 3) max stress is less than 0.05 GPa and 4) the displacement is less than 0.001 Å. We have confirmed the k-points of 2×2×4 for Cr, Fe, Co, Ni, Cu, Zn complexes, and 2×2×2 for $[Mn(DAT)_6](ClO_4)_2$. The cutoff energy of 900 eV has been set as for all the complexes in the optimization.

Table S5 The theoretical cell parameters of the optimized $[Cr(DAT)_6](ClO_4)_2$.

	$[Cr(DAT)_6](ClO_4)_2$		**coordinates**		
a (Å)	11.7917	N	0.07354	0.18010	0.30716
b(Å)	11.7917	N	0.20537	0.25881	0.26495
c(Å)	6.4497	N	0.23354	0.37604	0.20459
α(°)	90.0000	N	0.11580	0.37468	0.20542
β(°)	90.0000	N	0.09510	0.47622	0.14928
γ(°)	120.0000	H	0.14815	0.55650	0.24315
Symmetry	*P-3*	H	0.11894	0.50093	-0.00430
		N	-0.10652	0.22254	0.28063
		H	-0.12863	0.29418	0.24651
	x,y,z	H	-0.17792	0.12418	0.28715
	-y,x-y,z	C	0.01832	0.25434	0.26620
Symmetry code	-x+y,-x,z	O	0.58053	0.37843	0.29267
	-x,-y,-z	Cr	0.00000	0.00000	0.50000
	y,-x+y,-z	Cl	0.66667	0.33333	0.36634
	x-y,x,-z	O	0.66667	0.33333	0.58945

Table S6 The theoretical cell parameters of the optimized $[Mn(DAT)_6](ClO_4)_2$.

	$[Mn(DAT)_6](ClO_4)_2$		**coordinates**		
a (Å)	11.8435	N	0.18292	0.10596	0.15155
b(Å)	11.8435	N	0.26216	0.05383	0.13231
c(Å)	13.0810	N	0.37845	0.14299	0.10176
α(°)	90.0000	N	0.37551	0.25814	0.10032
β(°)	90.0000	N	0.47704	0.38054	0.07443
γ(°)	120.0000	H	0.50350	0.38276	-0.00104
Symmetry	P-3C1	H	0.55597	0.40702	0.12186
		N	0.22476	0.32767	0.14275
		H	0.12701	0.30176	0.14546
	x,y,z	H	0.29496	0.42082	0.12345
	-y,x-y,z	C	0.25604	0.23476	0.13155
Symmetry code	-x+y,-x,z	O	0.79766	0.37997	0.35660
	y,x,-z+1/2	Mn	0.00000	0.00000	0.25000
	x-y,-y,-z+1/2	Cl	0.66667	0.33333	0.32020
	-x,-x+y,-z+1/2	O	0.66667	0.33333	0.21015
	-x,-y,-z				
	y,-x+y,-z				
	x-y,x,-z				
	-y,-x,z+1/2				
	-x+y,y,z+1/2				
	x,x-y,z+1/2				

Table S7 The theoretical cell parameters of the optimized $[Fe(DAT)_6](ClO_4)_2$.

	$[Fe(DAT)_6](ClO_4)_2$		**coordinates**		
a (Å)	11.7755	N	0.17881	0.10579	0.31048
b(Å)	11.7755	N	0.25701	0.05217	0.26659
c(Å)	6.4476	N	0.37404	0.14066	0.20407
α(°)	90.0000	N	0.37331	0.25749	0.20516
β(°)	90.0000	N	0.47524	0.37967	0.14869
γ(°)	120.0000	H	0.55567	0.40651	0.24228
Symmetry	P-3	H	0.49962	0.38048	-0.00510
		N	0.22241	0.32899	0.28301
		H	0.29424	0.42244	0.24689
	x,y,z	H	0.12390	0.30210	0.29046
	-y,x-y,z	C	0.25335	0.23524	0.26805
Symmetry code	-x+y,-x,z	O	0.20196	0.58028	0.29263
	-x,-y,-z	Fe	0.00000	0.00000	0.50000
	y,-x+y,-z	Cl	0.33333	0.66667	0.36626
	x-y,x,-z	O	0.33333	0.66667	0.58954

Table S8 The theoretical cell parameters of the optimized $[Co(DAT)_6](ClO_4)_2$.

	$[Co(DAT)_6](ClO_4)_2$		**coordinates**		
a (Å)	11.7577	N	0.17772	0.10529	0.31203
b(Å)	11.7577	N	0.25478	0.05086	0.26415
c(Å)	6.4306	N	0.37169	0.13895	0.19944
α(°)	90.0000	N	0.37205	0.25645	0.20372
β(°)	90.0000	N	0.47430	0.37861	0.14689
γ(°)	120.0000	H	0.55539	0.40460	0.23893
Symmetry	P-3	H	0.49751	0.37989	-0.00797

		N	0.22309	0.32966	0.28819
		H	0.29522	0.42278	0.24969
	x,y,z	H	0.12432	0.30269	0.29275
	-y,x-y,z	C	0.25281	0.23500	0.27009
Symmetry code	-x+y,-x,z	O	0.20181	0.57972	0.29594
	-x,-y,-z	Co	0.00000	0.00000	0.50000
	y,-x+y,-z	Cl	0.33333	0.66667	0.36952
	x-y,x,-z	O	0.33333	0.66667	0.59348

Table S9 The theoretical cell parameters of the optimized $[Ni(DAT)_6](ClO_4)_2$.

	$[Ni(DAT)_6](ClO_4)_2$		**coordinates**		
a (Å)	11.7517	N	0.17534	0.10477	0.31283
b(Å)	11.7517	N	0.25137	0.04950	0.26382
c(Å)	6.4186	N	0.36868	0.13708	0.19928
α(°)	90.0000	N	0.37009	0.25507	0.20435
β(°)	90.0000	N	0.47311	0.37710	0.14815
γ(°)	120.0000	H	0.55376	0.40236	0.24121
Symmetry	P-3	H	0.49669	0.37834	-0.00682
		N	0.22298	0.33024	0.29119
		H	0.29545	0.42284	0.25085
	x,y,z	H	0.12423	0.30354	0.29386
	-y,x-y,z	C	0.25126	0.23454	0.27175
Symmetry code	-x+y,-x,z	O	0.20183	0.57967	0.29412
	-x,-y,-z	Ni	0.00000	0.00000	0.50000
	y,-x+y,-z	Cl	0.33333	0.66667	0.36785
	x-y,x,-z	O	0.33333	0.66667	0.59235

Table S10 The theoretical cell parameters of the optimized $[Cu(DAT)_6](ClO_4)_2$.

	$[Cu(DAT)_6](ClO_4)_2$		coordinates		
a (Å)	11.7741	N	0.17811	0.10566	0.30996
b(Å)	11.7741	N	0.25643	0.05226	0.26902
c(Å)	6.4382	N	0.37383	0.14074	0.20736
α(°)	90.0000	N	0.37288	0.25745	0.20701
β(°)	90.0000	N	0.47528	0.37980	0.15244
γ(°)	120.0000	H	0.55484	0.40654	0.24821
Symmetry	P-3	H	0.50115	0.38109	-0.00088
		N	0.22148	0.32889	0.28123
		H	0.29340	0.42228	0.24492
	x,y,z	H	0.12296	0.30190	0.28969
	-y,x-y,z	C	0.25251	0.23513	0.26809
Symmetry code	-x+y,-x,z	O	0.20190	0.58048	0.28758
	-x,-y,-z	Cu	0.00000	0.00000	0.50000
	y,-x+y,-z	Cl	0.33333	0.66667	0.36137
	x-y,x,-z	O	0.33333	0.66667	0.58485

Table S11 The theoretical cell parameters of the optimized $[Zn(DAT)_6](ClO_4)_2$.

	$[Zn(DAT)_6](ClO_4)_2$		coordinates		
a (Å)	11.7801	N	0.07322	0.17984	0.30852
b(Å)	11.7801	N	0.20490	0.25810	0.26635
c(Å)	6.4500	N	0.23336	0.37511	0.20397
α(°)	90.0000	N	0.11565	0.37406	0.20436
β(°)	90.0000	N	0.09520	0.47586	0.14827
γ(°)	120.0000	H	0.14888	0.55628	0.24172
Symmetry	P-3	H	0.11838	0.50024	-0.00554
		N	-0.10683	0.22247	0.28124
		H	-0.12878	0.29414	0.24588
	x,y,z	H	-0.17831	0.12402	0.28862
	-y,x-y,z	C	0.01802	0.25392	0.26659
Symmetry code	-x+y,-x,z	O	0.58022	0.37819	0.29394
	-x,-y,-z	Zn	0.00000	0.00000	0.50000
	y,-x+y,-z	Cl	0.66667	0.33333	0.36762
	x-y,x,-z	O	0.66667	0.33333	0.59081

3.2 Structural parameters based on the optimized crystals

Table S12 The band gaps, selected atomic charges, Metal stabilization energy (MSE), typical bond lengths and bond angles of $[Cr(DAT)_6](ClO_4)_2$.

$Cr(DAT)_6(ClO_4)_2$					
Band gap	0			**MSE(eV)**	-11.80
Charge(N1/N1a/N1b/M/N1c/N1d/N1e)				-0.13/-0.13/-0.13/0.40/-0.13/-0.13/-0.13	
Charge(C1/C1a/C1b/C1c/C1d/N1e)				0.13/0.13/0.13/0.13/0.13/0.13	
Charge(N2/N3/N4/N5)				-0.03/-0.05/0.05/-0.14	
M-N1(D/P)	2.24/0.13	**C1a-N1a(D/P)**	1.35/1.01	**N3-N4(D/P)**	1.38/0.68
M-N1a(D/P)	2.24/0.13	**C1c-N1c(D/P)**	1.35/1.01	**N4-N5(D/P)**	1.38/0.59
M-N1b(D/P)	2.24/0.13	**C1d-N1d(D/P)**	1.35/1.01	**Cl-O(D/P)**	1.44/0.43
M-N1c(D/P)	2.24/0.13	**C1e-N1e(D/P)**	1.35/1.01	**N1a-M-N1b(°)**	88.09
M-N1d(D/P)	2.24/0.13	**C1b-N1b(D/P)**	1.35/1.01	**N1b-M-N1c(°)**	91.91
M-N1e(D/P)	2.24/0.13	**C1-N4(D/P)**	1.36/0.93	**N1c-M-N1d(°)**	91.91
C1-N1(D/P)	1.35/1.01	**N2-N3(D/P)**	1.31/0.91	**N1d-M-N1e(°)**	88.09

Table S13 The band gaps, selected atomic charges, MSE, typical bond lengths and bond angles of $[Mn(DAT)_6](ClO_4)_2$.

$Mn(DAT)_6(ClO_4)_2$					
Band gap	2.15			**MSE (eV)**	-15.01
Charge(N1/N1a/N1b/M/N1c/N1d/N1e)				-0.11/-0.11/-0.11/0.32/-0.11/-0.11/-0.11	
Charge(C1/C1a/C1b/C1c/C1d/N1e)				0.13/0.13/0.13/0.13/0.13/0.13/	
Charge(N2/N3/N4/N5)				-0.03/-0.05/0.05/-0.14	
M-N1(D/P)	2.28/0.19	**C1a-N1a(D/P)**	1.35/1.01	**N3-N4(D/P)**	1.38/0.68
M-N1a(D/P)	2.28/0.19	**C1b-N1b(D/P)**	1.35/1.01	**N4-N5(D/P)**	1.38/0.59
M-N1b(D/P)	2.28/0.19	**C1c-N1c(D/P)**	1.35/1.01	**Cl-O(D/P)**	1.44/0.42
M-N1c(D/P)	2.28/0.19	**C1d-N1d(D/P)**	1.35/1.01	**N1-M-N1a(°)**	95.20
M-N1d(D/P)	2.28/0.19	**C1e-N1e(D/P)**	1.35/1.01	**N1a-M-N1b(°)**	82.87
M-N1e(D/P)	2.28/0.19	**C1-N4(D/P)**	1.36/0.93	**N1b-M-N1c(°)**	95.20
C1-N1(D/P)	1.35/1.01	**N2-N3(D/P)**	1.30/0.90	**N1c-M-N1d(°)**	82.87

Table S14 The band gaps, selected atomic charges, MSE, typical bond lengths and bond angles of $[Fe(DAT)_6](ClO_4)_2$.

$Fe(DAT)_6(ClO_4)_2$					
Band gap	0			**MSE(eV)**	-17.81
Charge(N1/N1a/N1b/M/N1c/N1d/N1e)				-0.10/-0.10/-0.10/0.27/-0.10/-0.10/-0.10	
Charge(C1/C1a/C1b/C1c/C1d/N1e)				0.13/0.13/0.13/0.13/0.13/0.13	
Charge(N2/N3/N4/N5)				-0.03/-0.05/0.05/-0.14	
M-N1(D/P)	2.23/0.19	**C1a-N1a(D/P)**	1.35/1.00	**N3-N4(D/P)**	1.38/0.68
M-N1a(D/P)	2.23/0.19	**C1b-N1b(D/P)**	1.35/1.00	**N4-N5(D/P)**	1.38/0.60
M-N1b(D/P)	2.23/0.19	**C1c-N1c(D/P)**	1.35/1.00	**Cl-O(D/P)**	1.44/0.43
M-N1c(D/P)	2.23/0.19	**C1d-N1d(D/P)**	1.35/1.00	**N1-M-N1a(°)**	89.05
M-N1d(D/P)	2.23/0.19	**C1e-N1e(D/P)**	1.35/1.00	**N1a-M-N1b(°)**	90.95
M-N1e(D/P)	2.23/0.19	**C1-N4(D/P)**	1.36/0.93	**N1b-M-N1c(°)**	90.95
C1-N1(D/P)	1.35/1.00	**N2-N3(D/P)**	1.31/0.91	**N1c-M-N1d(°)**	89.05

Table S15 The band gaps, selected atomic charges, MSE, typical bond lengths and bond angles of $[Co(DAT)_6](ClO_4)_2$.

$Co(DAT)_6(ClO_4)_2$					
Band gap	0.51			**MSE (eV)**	-14.46
Charge(N1/N1a/N1b/M/N1c/N1d/N1e)				-0.10/-0.10/-0.10/0.24/-0.10/-0.10/-0.10	
Charge(C1/C1a/C1b/C1c/C1d/N1e)				0.13/0.13/0.13/0.13/0.13/0.13	
Charge(N2/N3/N4/N5)				-0.02/-0.05/0.05/-0.14	
M-N1(D/P)	2.20/0.20	**C1a-N1a(D/P)**	1.35/1.00	**N4-N5(D/P)**	1.38/0.60
M-N1a(D/P)	2.20/0.20	**C1b-N1b(D/P)**	1.35/1.00	**Cl-O(D/P)**	1.44/0.43
M-N1b(D/P)	2.20/0.20	**C1d-N1d(D/P)**	1.35/1.00	**N1-M-N1a(°)**	91.67
M-N1c(D/P)	2.20/0.20	**C1e-N1e(D/P)**	1.35/1.00	**N1a-M-N1b(°)**	88.33
M-N1d(D/P)	2.20/0.20	**C1-N4(D/P)**	1.36/0.93	**N1b-M-N1c(°)**	91.67
M-N1e(D/P)	2.20/0.20	**N2-N3(D/P)**	1.31/0.91	**N1c-M-N1d(°)**	91.67
C1-N1(D/P)	1.35/1.00	**N3-N4(D/P)**	1.38/0.68	**N1d-M-N1e(°)**	88.33

Table S16 The band gaps, selected atomic charges, MSE, typical bond lengths and bond angles of $[Ni(DAT)_6](ClO_4)_2$.

$Ni(DAT)_6(ClO_4)_2$					
Band gap	1.63			**MSE (eV)**	-15.55
Charge(N1/N1a/N1b/M/N1c/N1d/N1e)				-0.09/-0.09/-0.09/0.20/-0.09/-0.09/-0.09	
Charge(C1/C1a/C1b/C1c/C1d/N1e)				0.13/0.13/0.13/0.13/0.13/0.13/	
Charge(N2/N3/N4/N5)				-0.02/-0.05/0.05/-0.14	
M-N1(D/P)	2.17/0.22	**C1a-N1a(D/P)**	1.35/1.01	**N3-N4(D/P)**	1.38/0.68
M-N1a(D/P)	2.17/0.22	**C1b-N1b(D/P)**	1.35/1.01	**N4-N5(D/P)**	1.38/0.60
M-N1b(D/P)	2.17/0.22	**C1c-N1c(D/P)**	1.35/1.01	**Cl-O(D/P)**	1.44/0.43
M-N1c(D/P)	2.17/0.22	**C1d-N1d(D/P)**	1.35/1.01	**N1-M-N1a(°)**	87.86
M-N1d(D/P)	2.17/0.22	**C1e-N1e(D/P)**	1.35/1.01	**N1a-M-N1b(°)**	92.14
M-N1e(D/P)	2.17/0.22	**C1-N4(D/P)**	1.36/0.93	**N1b-M-N1c(°)**	92.14
C1-N1(D/P)	1.35/1.01	**N2-N3(D/P)**	1.31/0.91	**N1c-M-N1d(°)**	87.86

Table S17 The band gaps, selected atomic charges, MSE, typical bond lengths and bond angles of $[Cu(DAT)_6](ClO_4)_2$.

$Cu(DAT)_6(ClO_4)_2$					
Band gap	0			**MSE (eV)**	-12.00
charge(N1/N1a/N1b/M/N1c/N1d/N1e)				-0.12/-0.12/-0.12/0.38/-0.12/-0.12/-0.12	
charge(C1/C1a/C1b/C1c/C1d/N1e)				0.13/0.13/0.13/0.13/0.13/0.13	
charge(N2/N3/N4/N5)				-0.02/-0.05/0.05/-0.14	
M-N1(D/P)	2.20/0.15	**C1a-N1a(D/P)**	1.35/1.01	**N3-N4(D/P)**	1.38/0.68
M-N1a(D/P)	2.20/0.15	**C1b-N1b(D/P)**	1.35/1.01	**N4-N5(D/P)**	1.38/0.60
M-N1b(D/P)	2.20/0.15	**C1c-N1c(D/P)**	1.35/1.01	**Cl-O(D/P)**	1.44/0.43
M-N1c(D/P)	2.20/0.15	**C1d-N1d(D/P)**	1.35/1.01	**N1-M-N1a(°)**	88.01
M-N1d(D/P)	2.20/0.15	**C1e-N1e(D/P)**	1.35/1.01	**N1a-M-N1b(°)**	91.99
M-N1e(D/P)	2.20/0.15	**C1-N4(D/P)**	1.36/0.93	**N1b-M-N1c(°)**	91.99
C1-N1(D/P)	1.35/1.01	**N2-N3(D/P)**	1.31/0.91	**N1c-M-N1d(°)**	88.01

Table S18 The band gaps, selected atomic charges, MSE, typical bond lengths and bond angles of $[Zn(DAT)_6](ClO_4)_2$.

$Zn(DAT)_6(ClO_4)_2$					
Band gap	3.59			**MSE(eV)**	-13.62 eV
charge(N1/N1a/N1b/M/N1c/N1d/N1e)				-0.12/-0.12/-0.12/0.40/-0.12/-0.12/-0.12	
charge(C1/C1a/C1b/C1c/C1d/N1e)				0.13/0.13/0.13/0.13/0.13/0.13	
charge(N2/N3/N4/N5)				-0.03/-0.05/0.05/-0.14	
M-N1(D/P)	2.22/0.21	**C1a-N1a(D/P)**	1.35/1.01	**N3-N4(D/P)**	1.38/0.68
M-N1a(D/P)	2.22/0.21	**C1b-N1b(D/P)**	1.35/1.01	**N4-N5(D/P)**	1.38/0.60
M-N1b(D/P)	2.22/0.21	**C1c-N1c(D/P)**	1.35/1.01	**Cl-O(D/P)**	1.44/0.43
M-N1c(D/P)	2.22/0.21	**C1d-N1d(D/P)**	1.35/1.01	**N1-M-N1a(°)**	87.71
M-N1d(D/P)	2.22/0.21	**C1e-N1e(D/P)**	1.35/1.01	**N1a-M-N1b(°)**	92.29
M-N1e(D/P)	2.22/0.21	**C1-N4(D/P)**	1.36/0.93	**N1b-M-N1c(°)**	92.29
C1-N1(D/P)	1.35/1.01	**N2-N3(D/P)**	1.31/0.92	**N1c-M-N1d(°)**	87.71

3.3 Density of States and partial density of states

We performed the Density of states and partial density of states for the seven complexes based on the optimized structures.

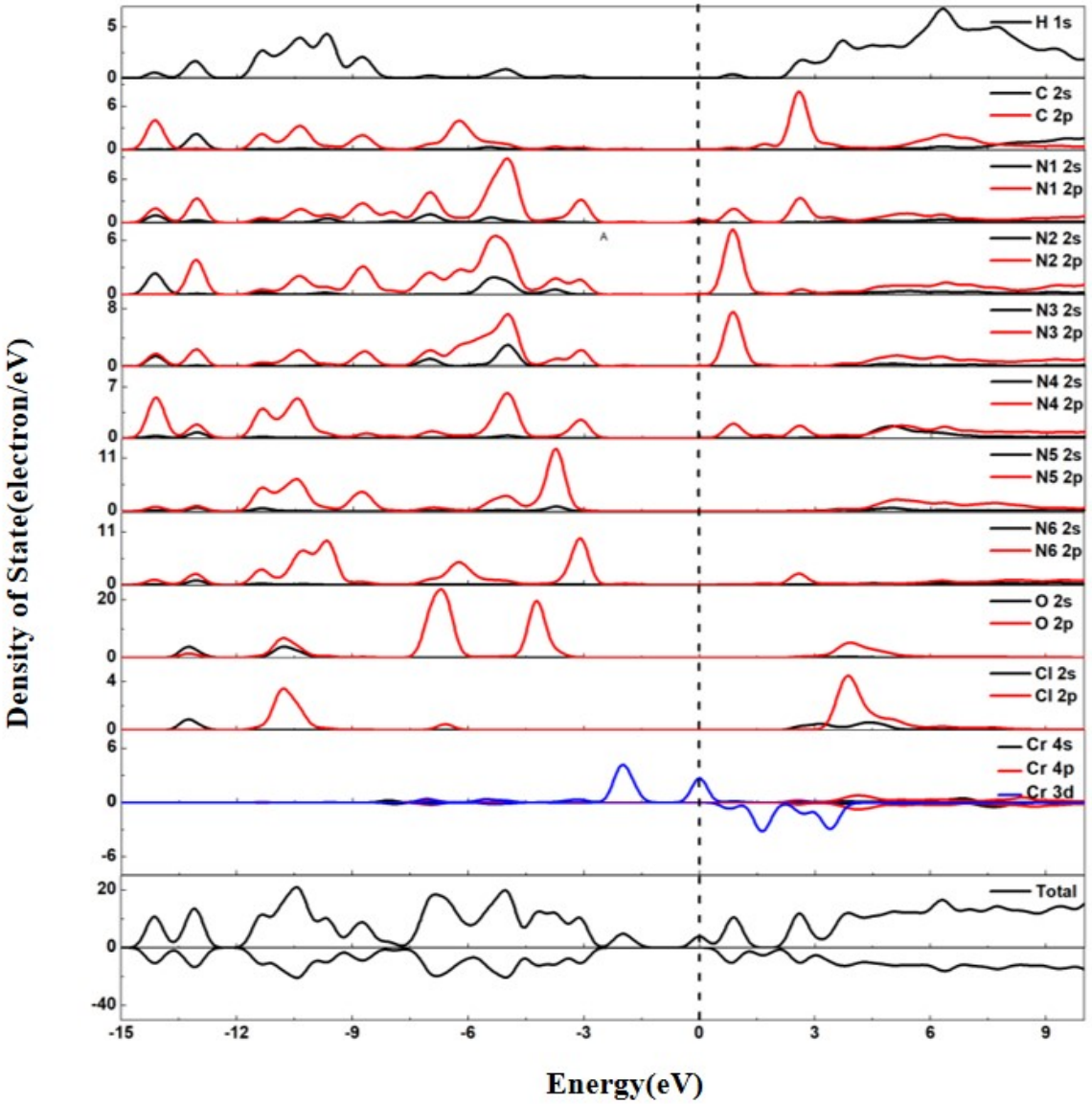

Figure S1 The density of states (DOS) and partial density of states (pDOS) of $[Cr(DAT)_6](ClO_4)_2$.

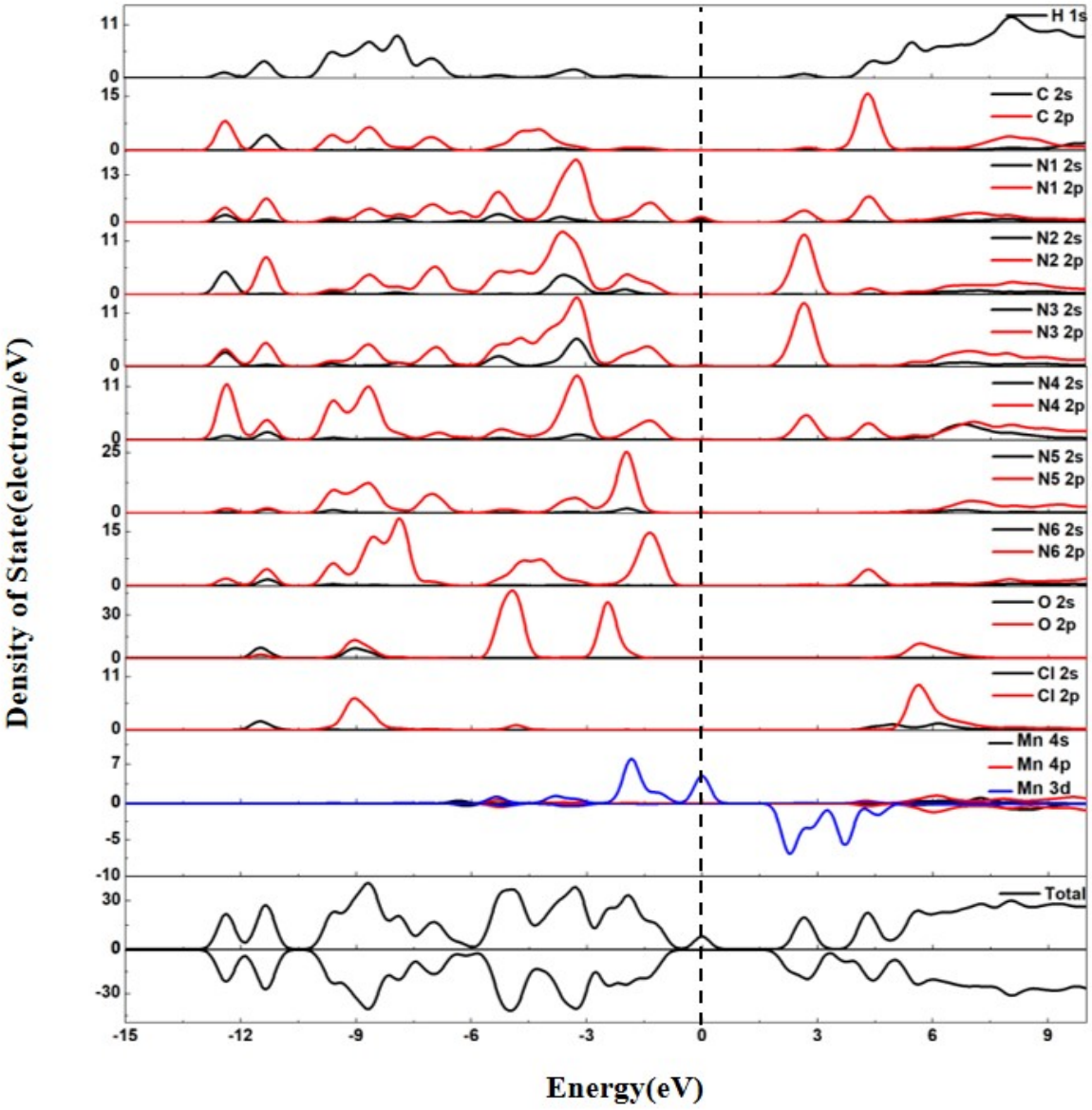

Figure S2 The density of states (DOS) and partial density of states (pDOS) of $[Mn(DAT)_6](ClO_4)_2$.

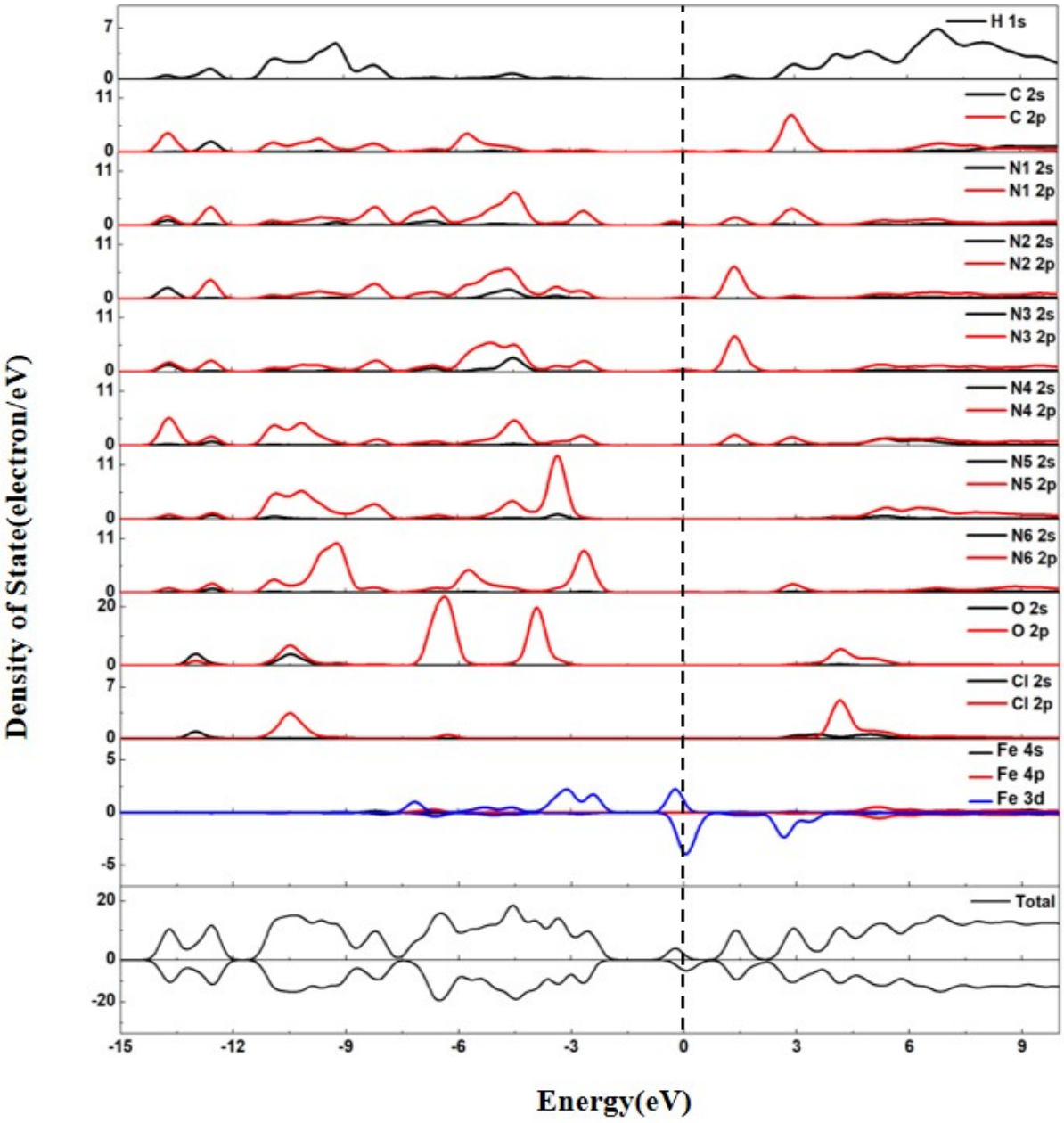

Figure S3. The density of states (DOS) and partial density of states (pDOS) of $[Fe(DAT)_6](ClO_4)_2$.

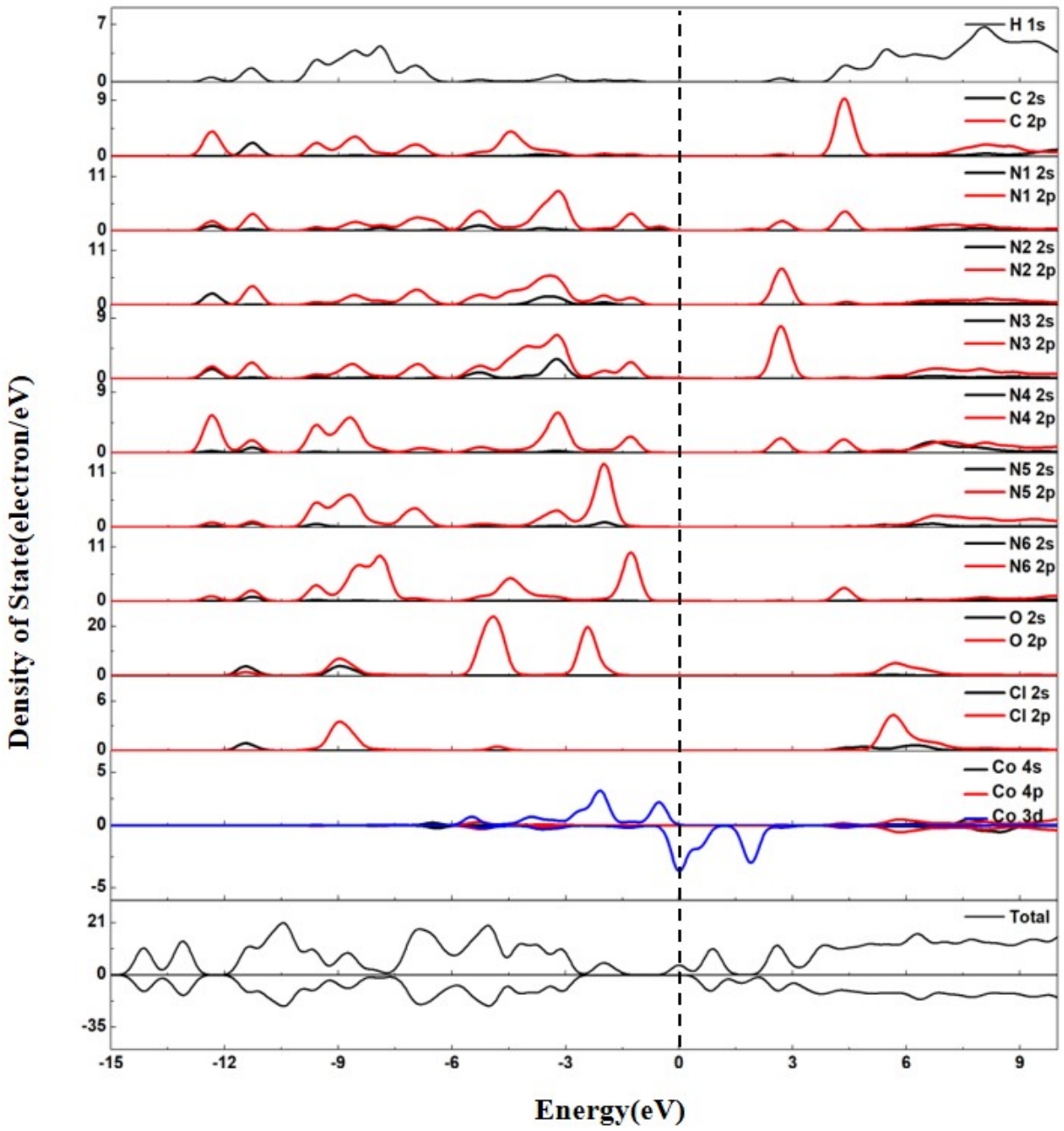

Figure S4. The density of states (DOS) and partial density of states (pDOS) of $[Co(DAT)_6](ClO_4)_2$.

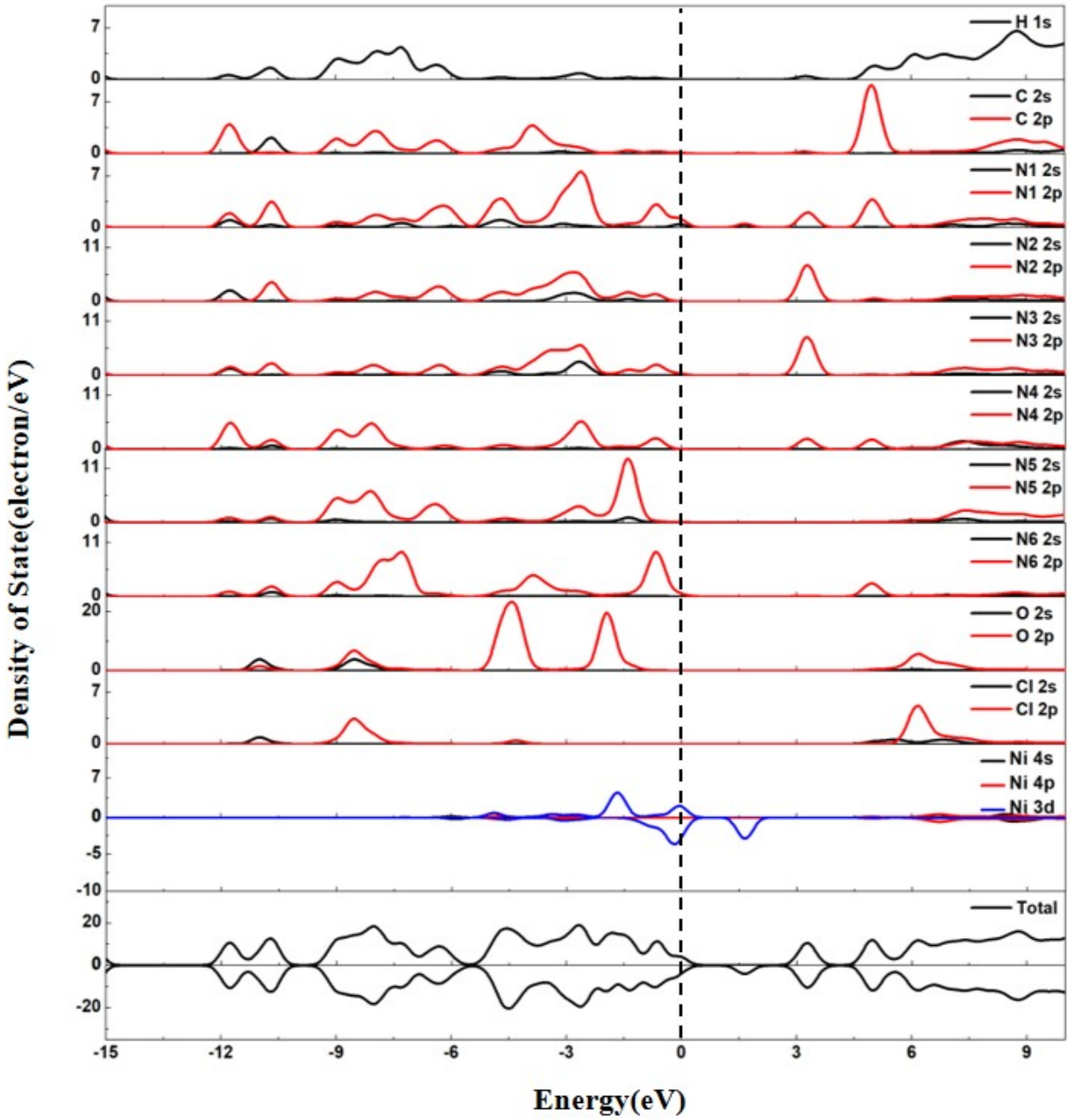

Figure S5. The density of states (DOS) and partial density of states (pDOS) of $[Ni(DAT)_6](ClO_4)_2$.

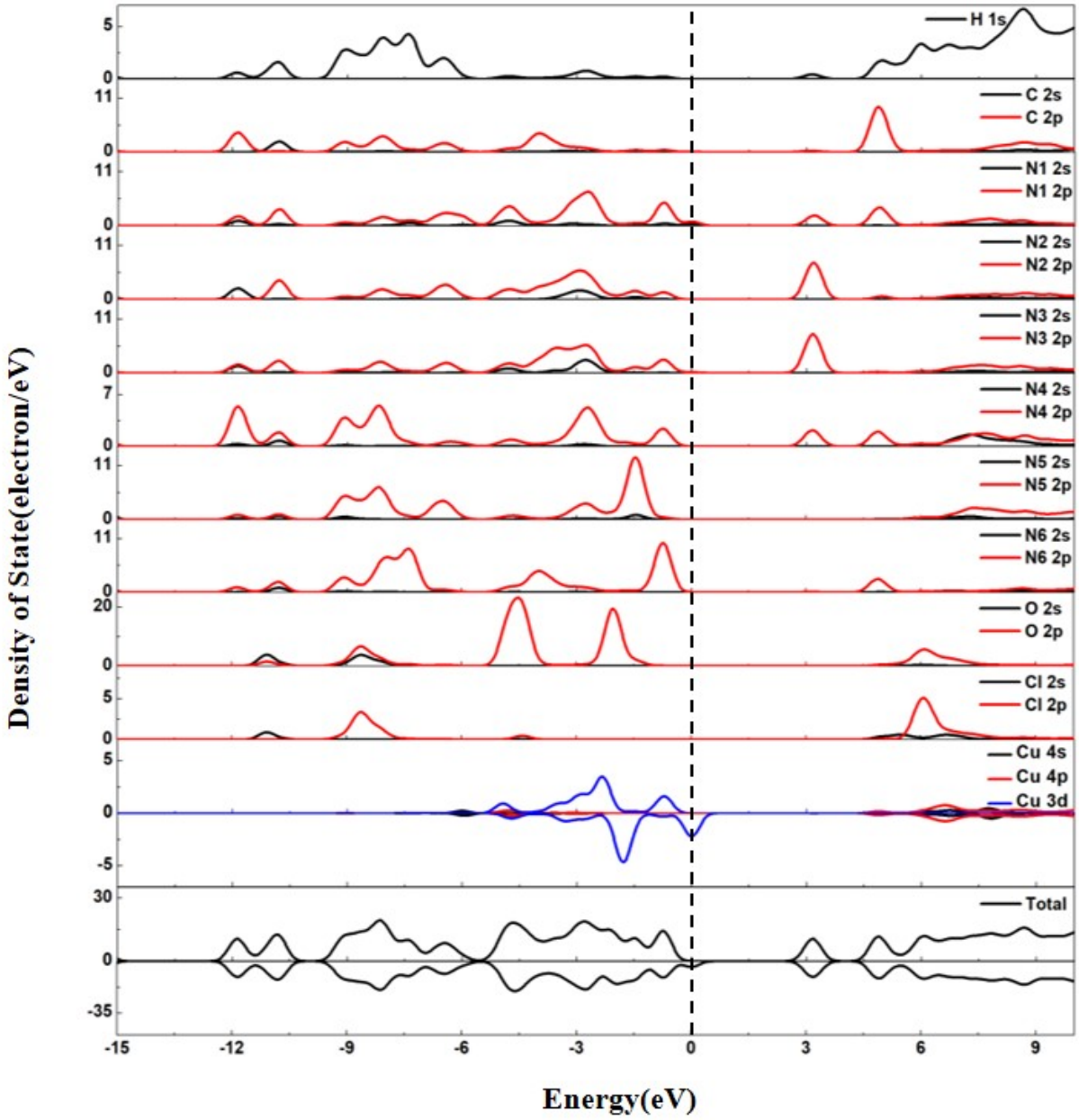

Figure S6. The density of states (DOS) and partial density of states (pDOS) of $[Cu(DAT)_6](ClO_4)_2$.

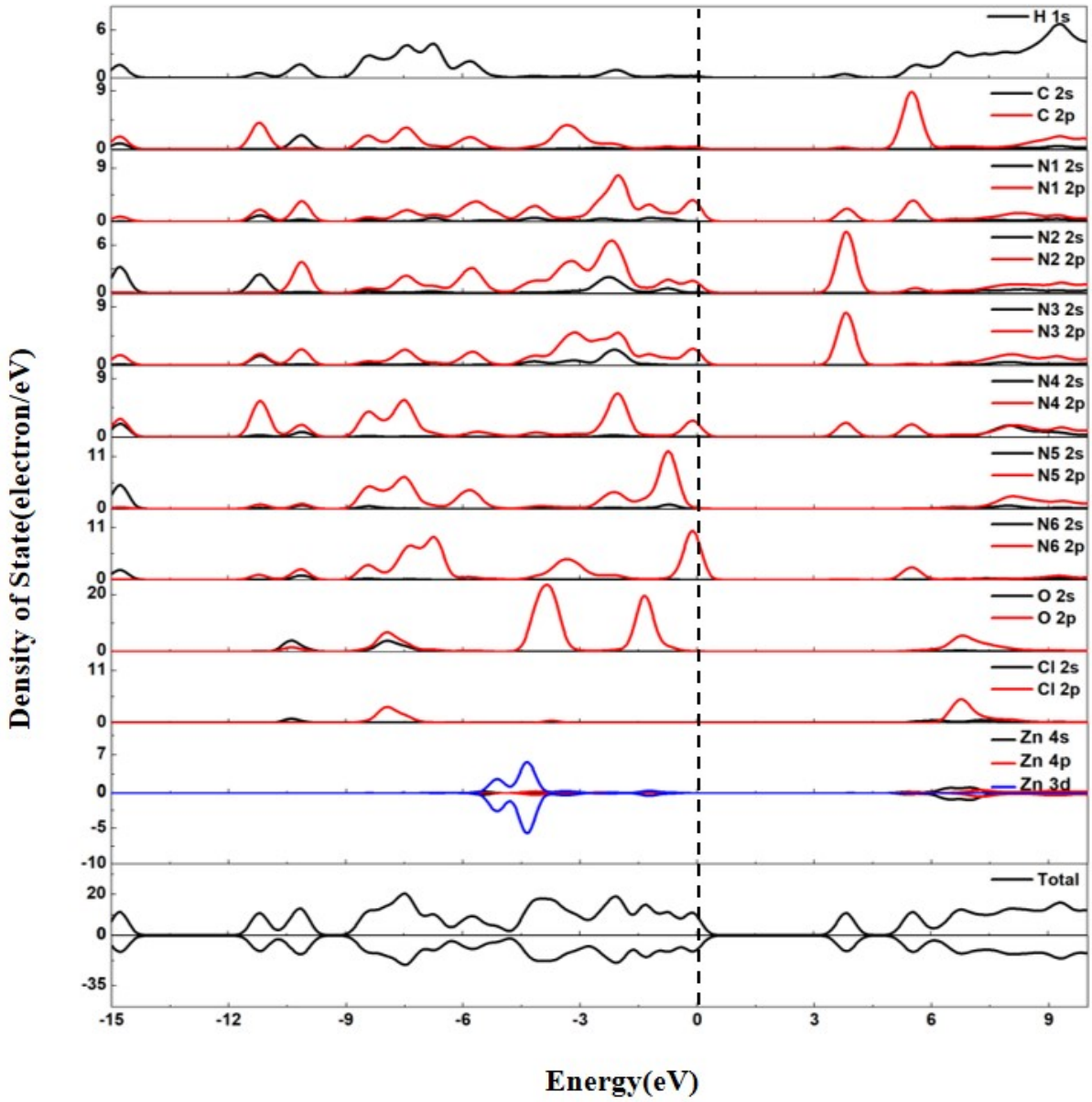

Figure S7. The density of states (DOS) and partial density of states (pDOS) of $[Zn(DAT)_6](ClO_4)_2$.

Section 4 CPMD simulations

4.1 Convergence curves of the temperature, virtual kinetic energies of electrons and the total electronic energies

The convergence statements suggest the equilibrium of the system before increasing the temperature, which is a necessary step in the molecular dynamic study. In this step, we initialize both the electronic and ionic velocities to zero to conserve the total energy and stay close to the Born-Oppenheimer surface.

In addition, the atomic force should converge to an appropriate range (around 10^{-3} atomic units) on the basis of the ground state structure. With the increased temperature, the system tends to equilibrium under the Nose's thermostats. We put the convergence of temperature of ions (T_{ions}), kinetic energies of virtual electrons (E_{kinc}) and the total electronic energies (E_{tot}) in Figure S8~ S14, indicating our systems have been relaxed enough for the preparation of CPMD study.

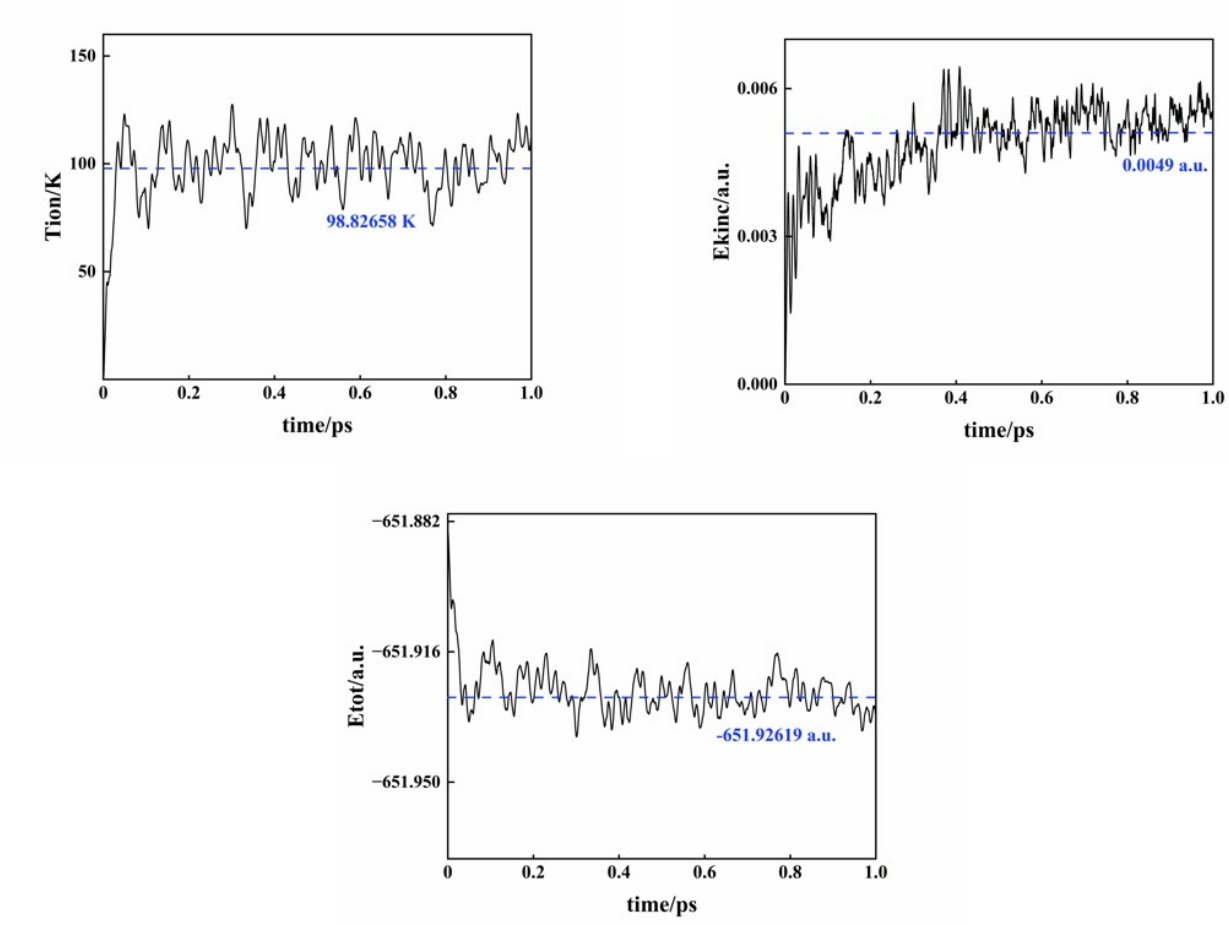

Figure S8. The convergence curves of the temperature of ions (T_{ions}), kinetic energies of virtual electrons (E_{kinc}) and the total electronic energies (E_{tot}) of $[Cr(DAT)_6](ClO_4)_2$.

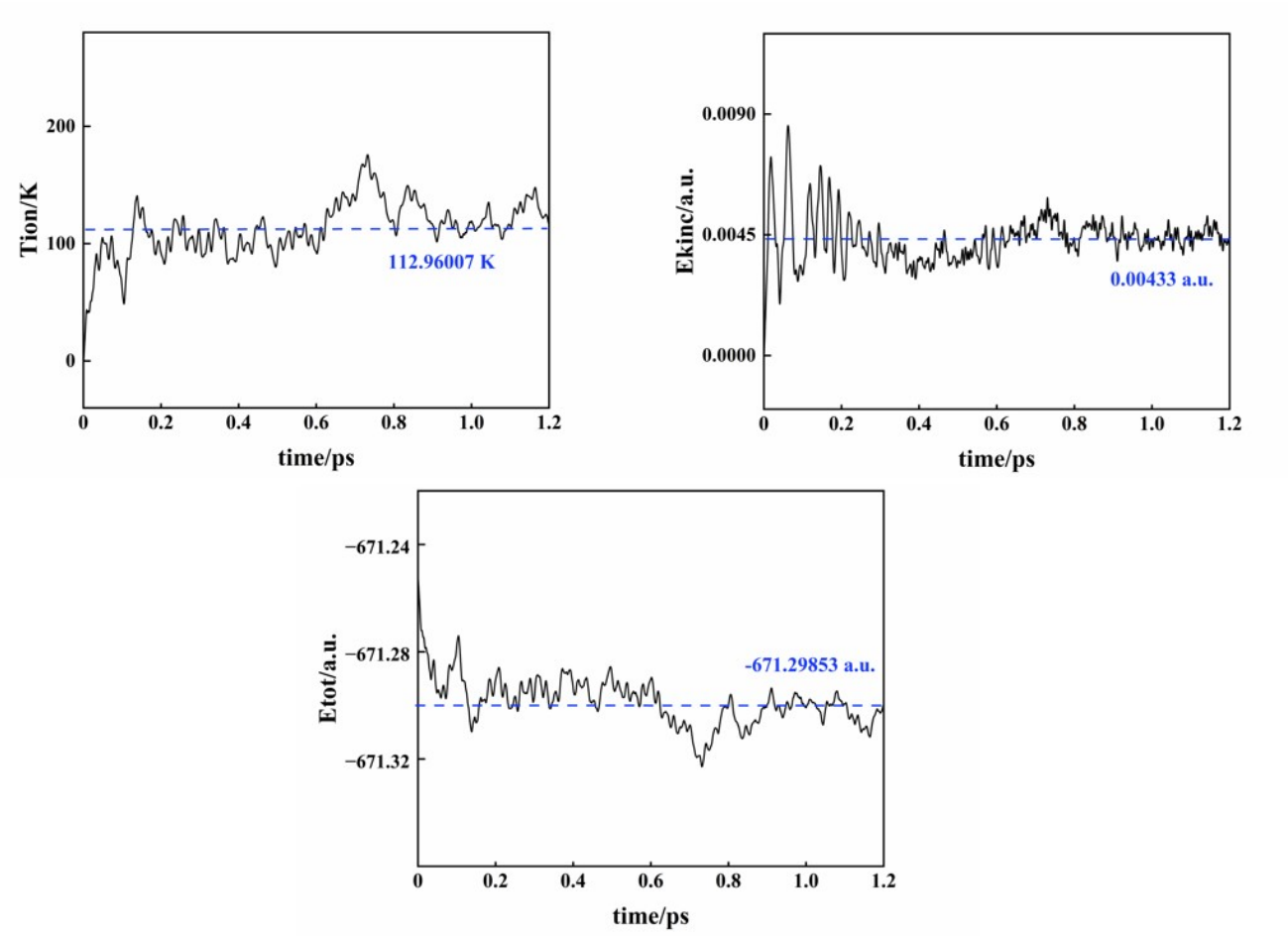

Figure S9. The convergence curves of the temperature of ions (T_{ions}), kinetic energies of virtual electrons (E_{kinc}) and the total electronic energies (E_{tot}) of $[Mn(DAT)_6](ClO_4)_2$.

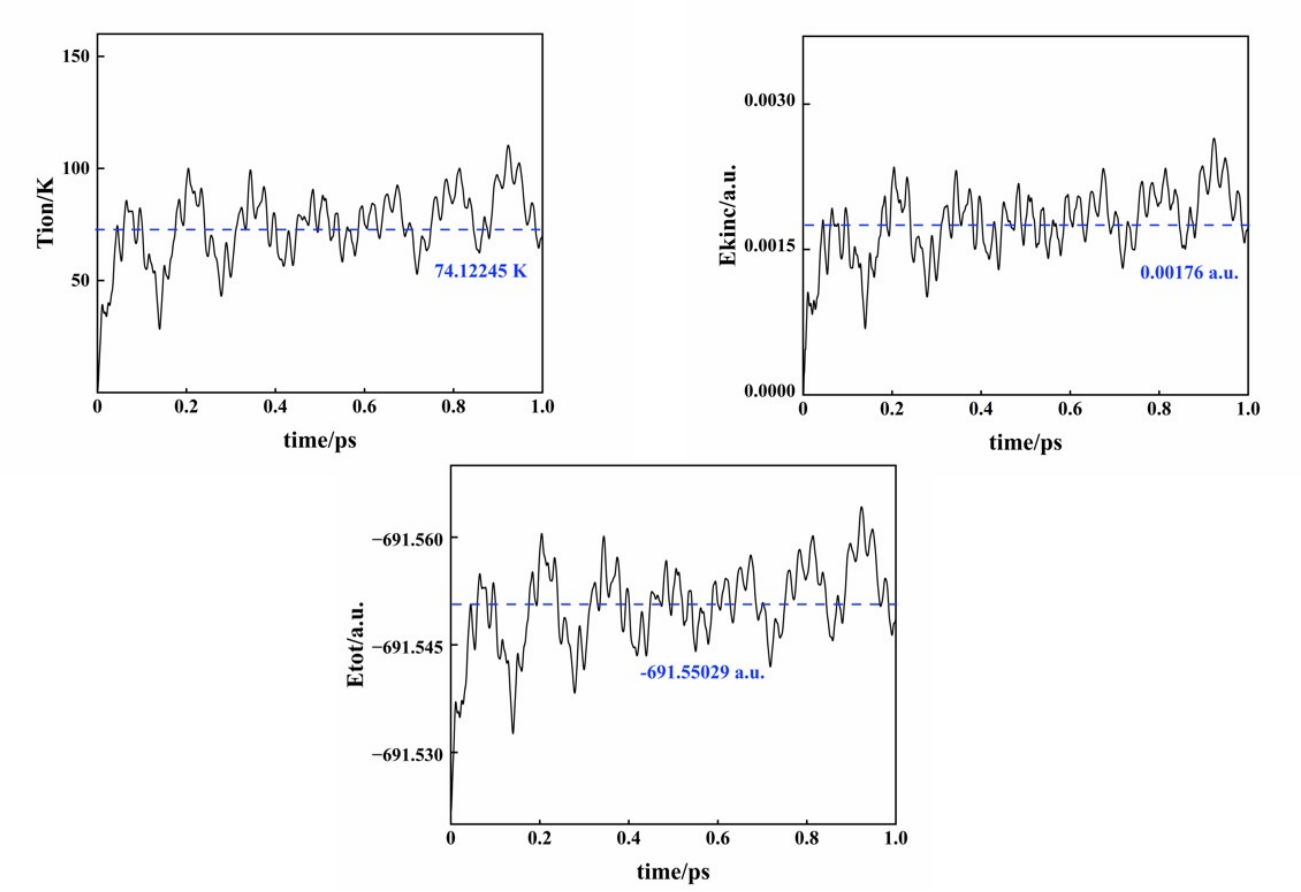

Figure S10. The convergence curves of the temperature of ions (T_{ions}), kinetic energies of virtual electrons (E_{kinc}) and the total electronic energies (E_{tot})of $[Fe(DAT)_6](ClO_4)_2$.

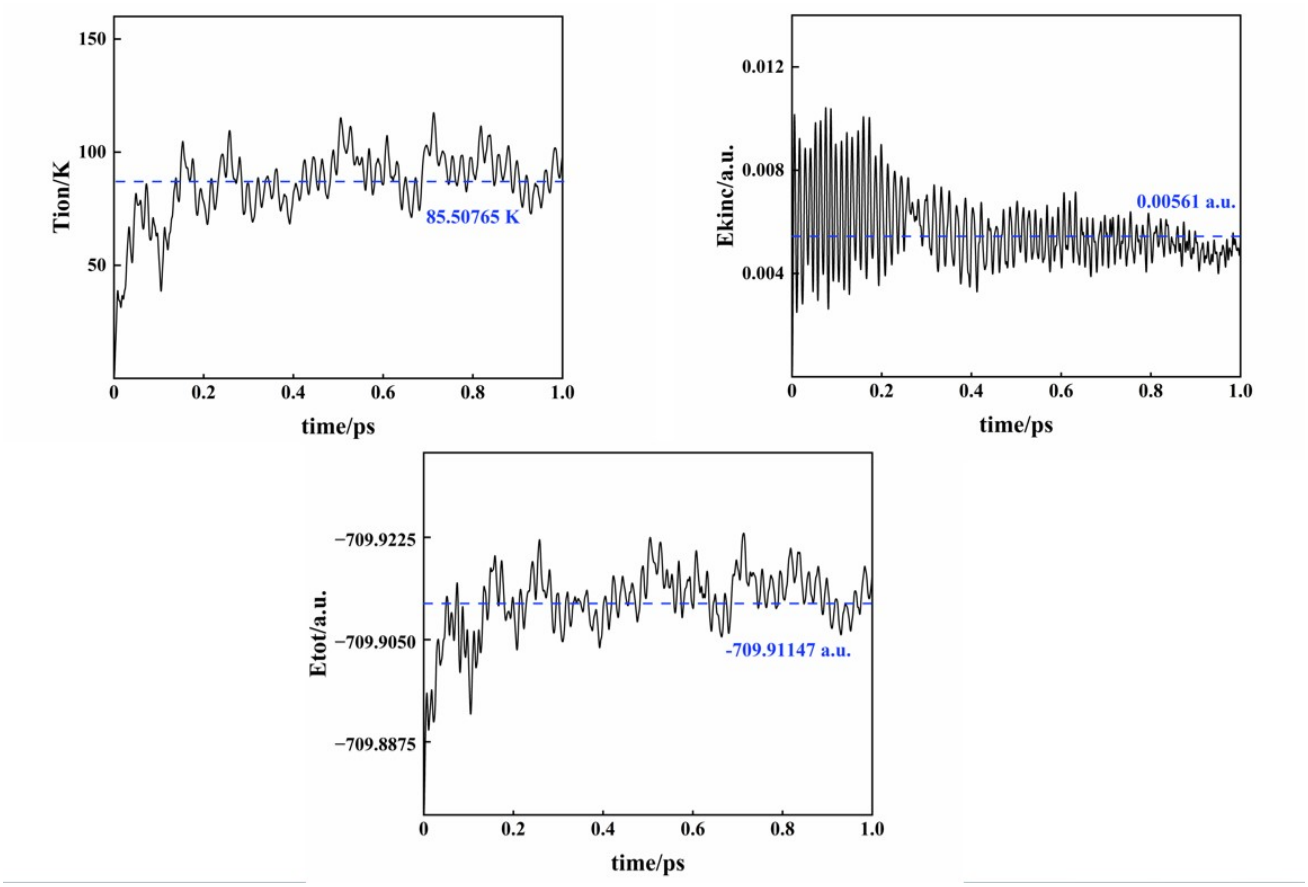

Figure S11. The convergence curves of the temperature of ions (Tions), kinetic energies of virtual electrons (Ekinc) and the total electronic energies (Etot) of $[Co(DAT)_6](ClO_4)_2$.

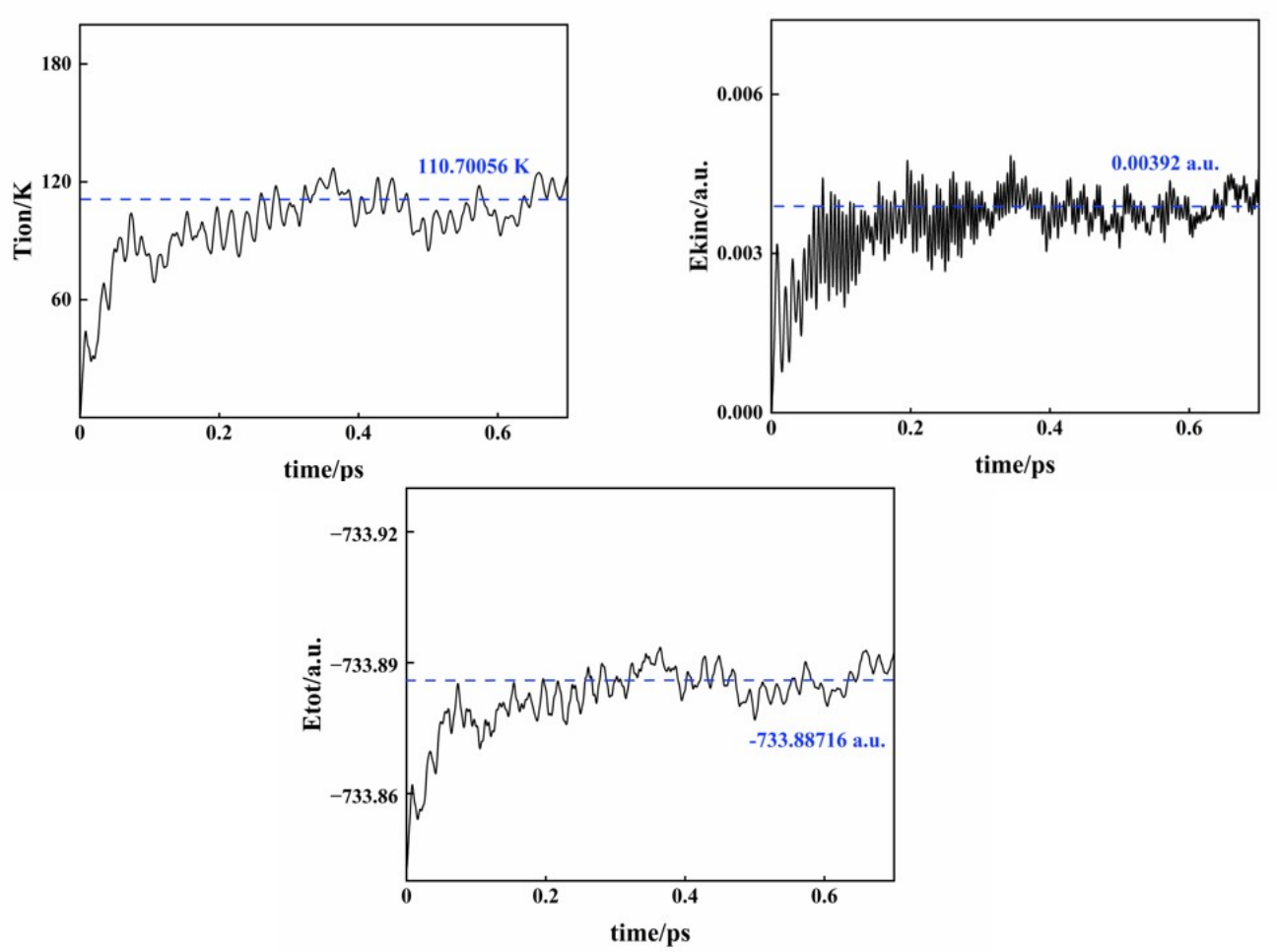

Figure S12. The convergence curves of the temperature of ions (T_{ions}), kinetic energies of virtual electrons (E_{kinc}) and the total electronic energies (E_{tot}) of $[Ni(DAT)_6](ClO_4)_2$.

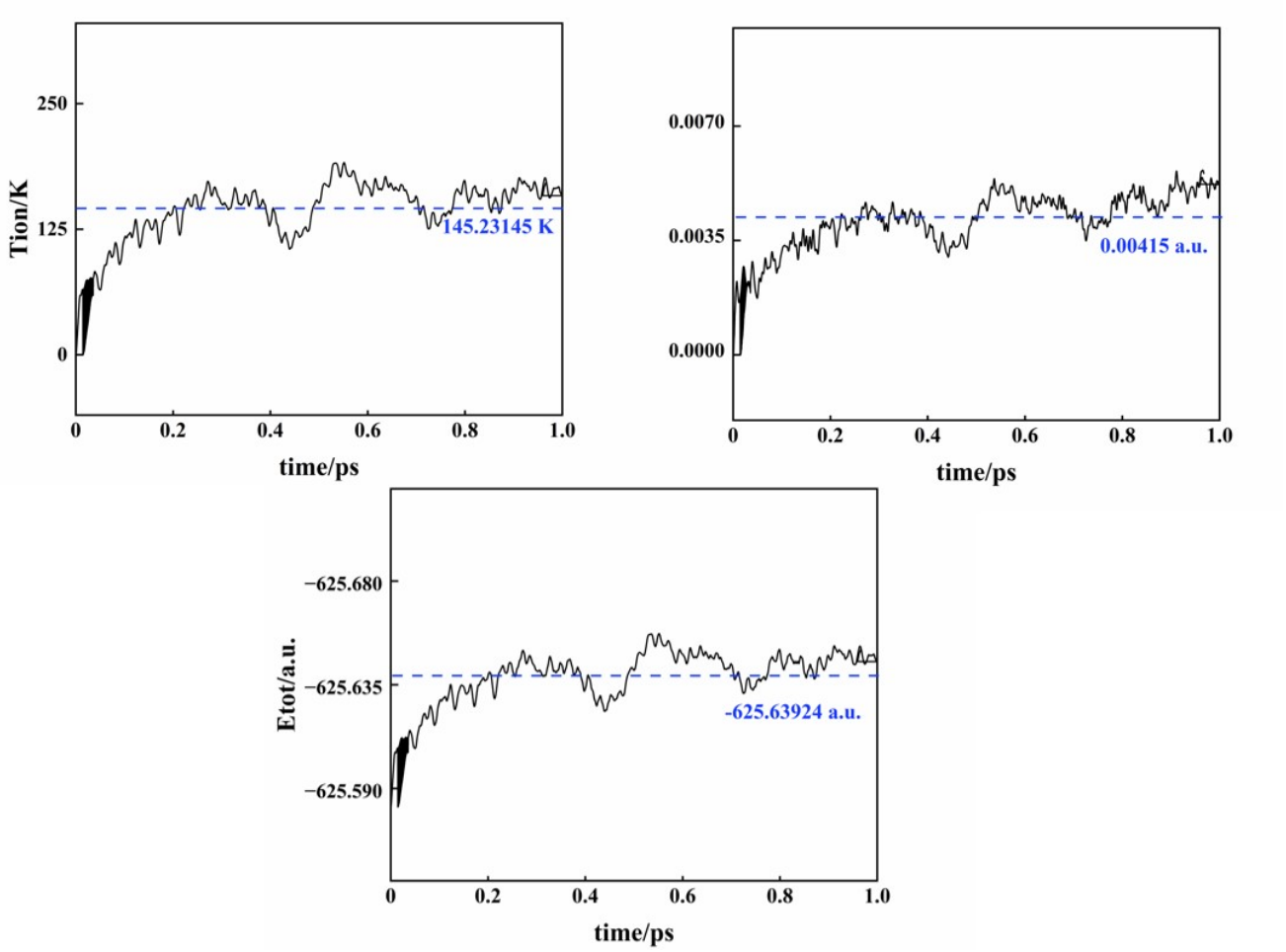

Figure S13. The convergence curves of the temperature of ions (T_{ions}), kinetic energies of virtual electrons (E_{kinc}) and the total electronic energies (E_{tot}) of $[Cu(DAT)_6](ClO_4)_2$.

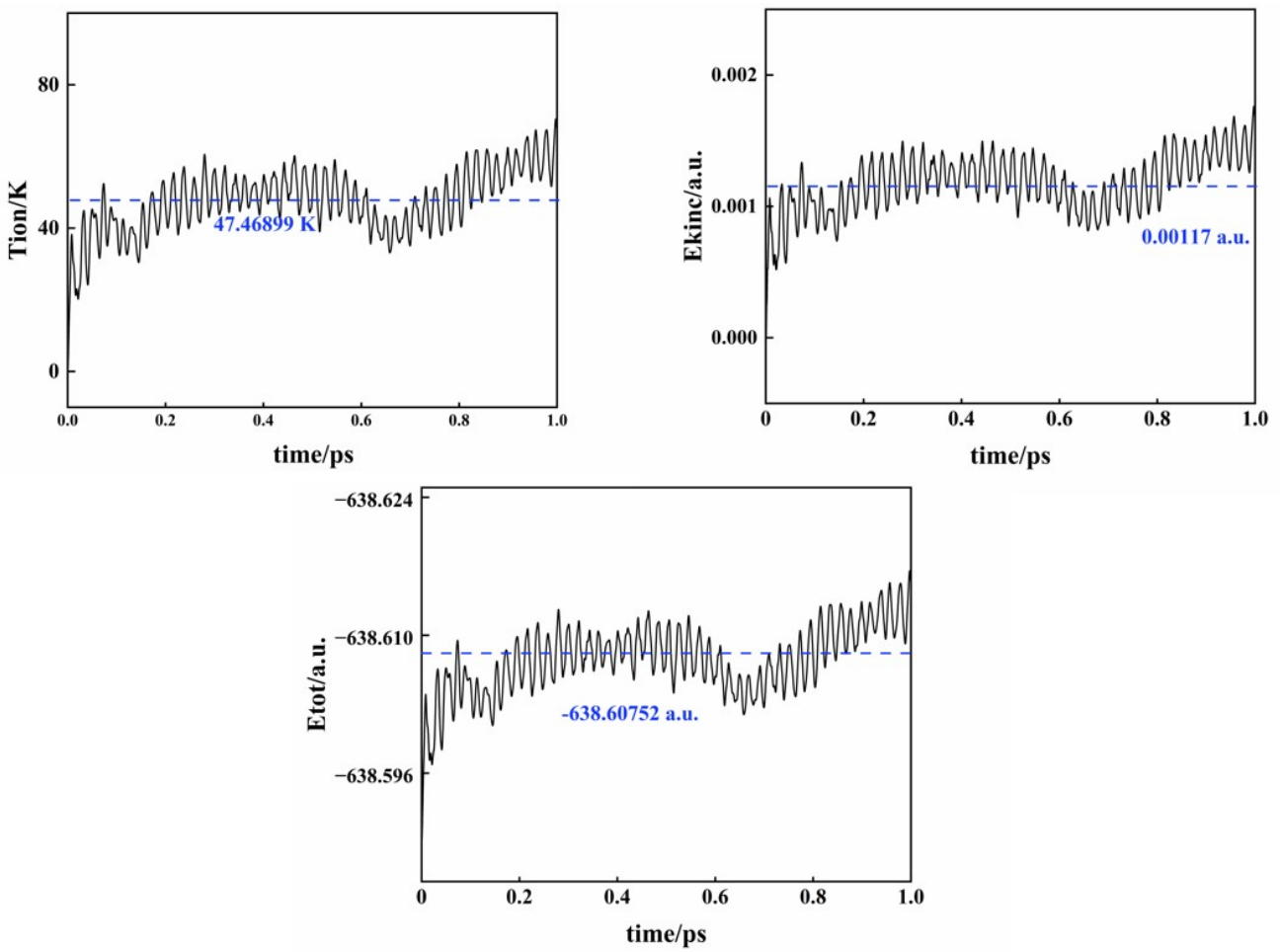

Figure S14. The convergence curves of the temperature of ions (T_{ions}), kinetic energies of virtual electrons (E_{kinc}) and the total electronic energies (E_{tot}) of $[Zn(DAT)_6](ClO_4)_2$.

4.2 The snapshots of the ignition and chain growth steps

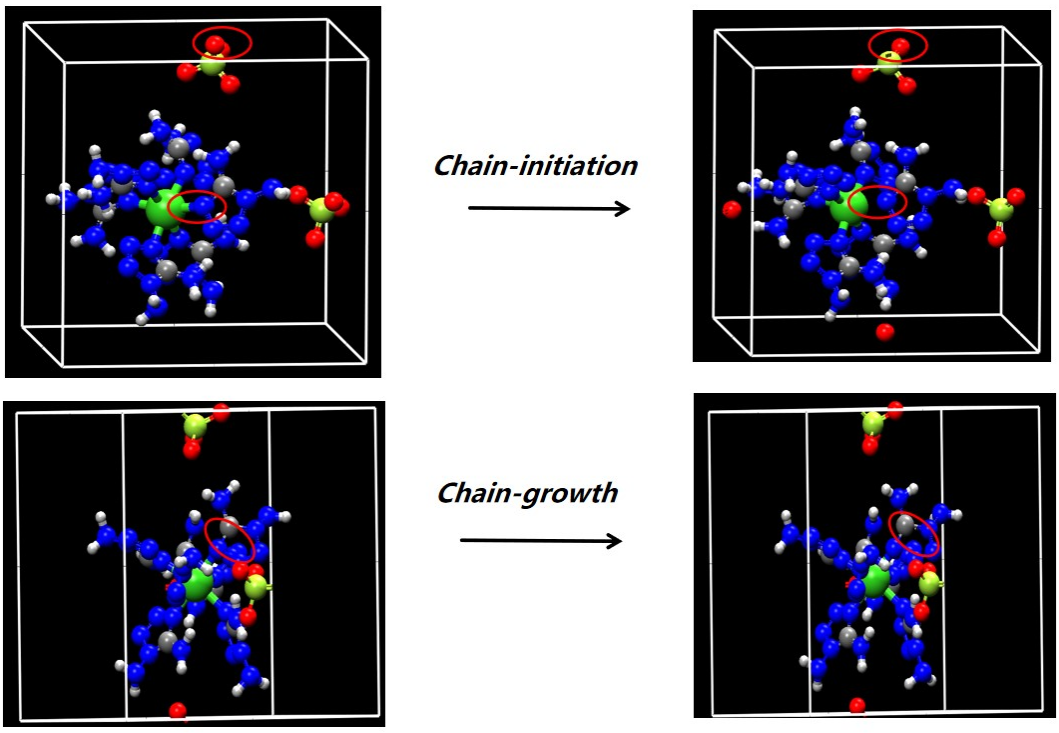

Figure S15. The snapshots of the chain initiation and chain growth process of $[Cr(DAT)_6](ClO_4)_2$.

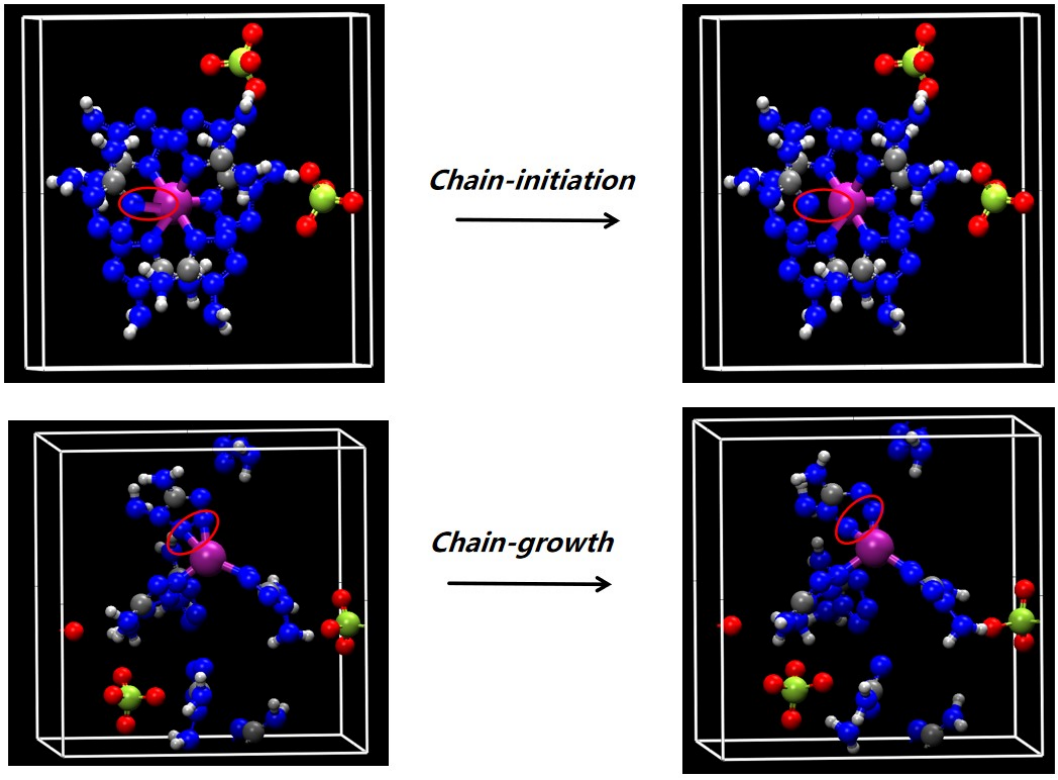

Figure S16. The snapshots of the chain initiation and chain growth process of $[Mn(DAT)_6](ClO_4)_2$.

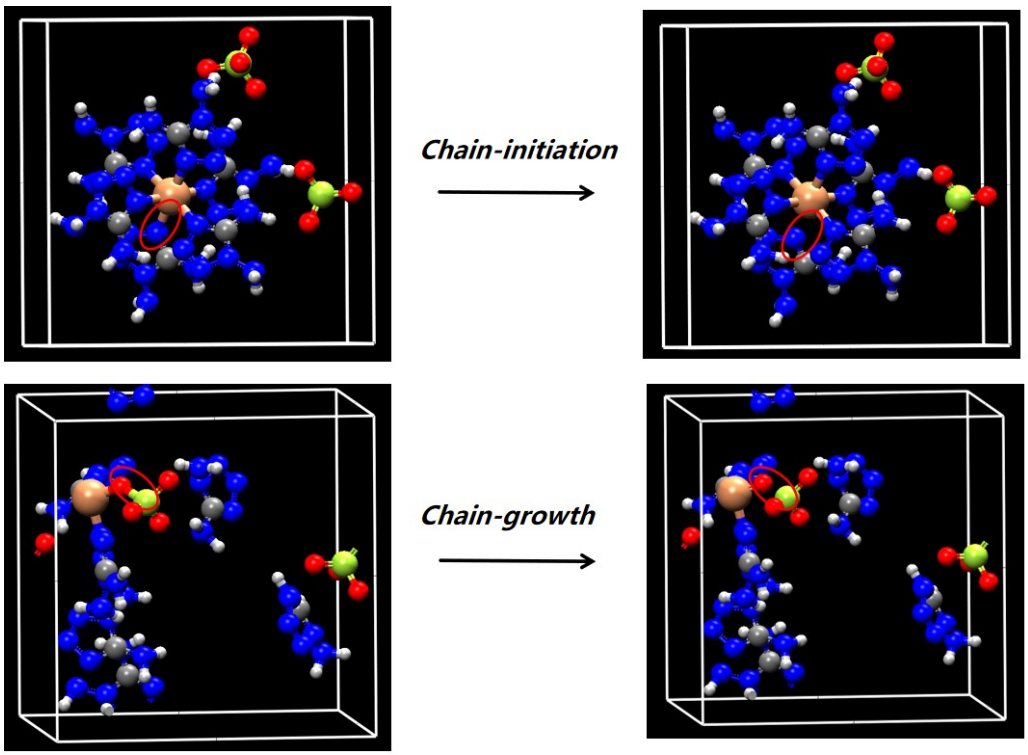

Figure S17. The snapshots of the chain initiation and chain growth process of $[Fe(DAT)_6](ClO_4)_2$.

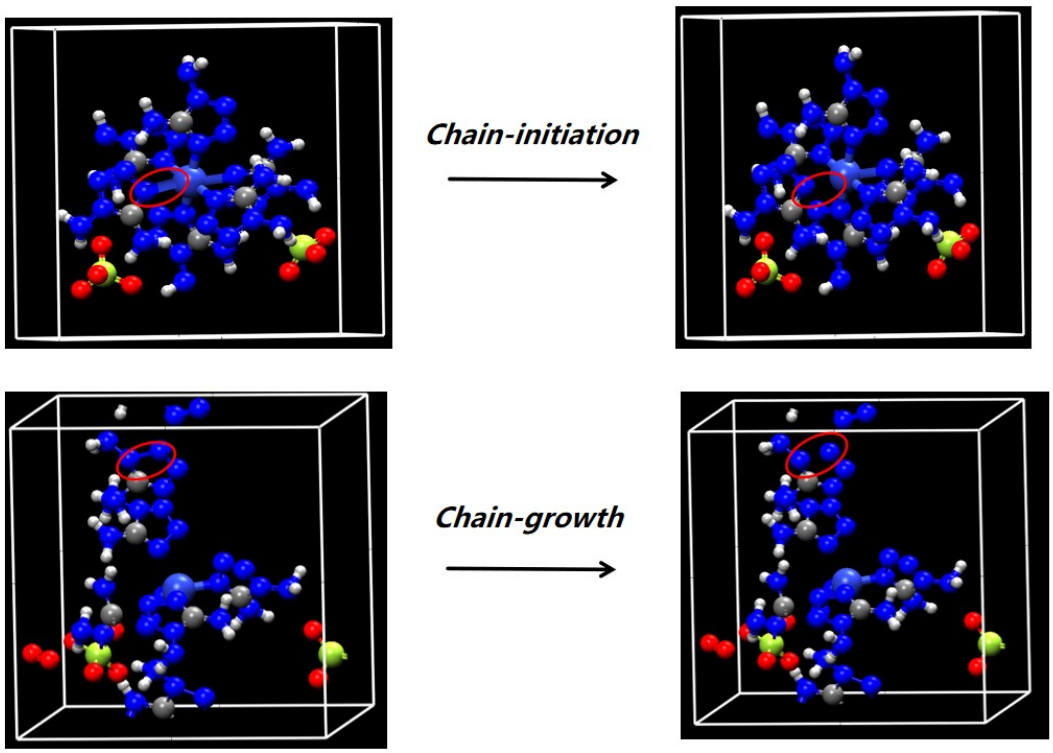

Figure S18. The snapshots of the chain initiation and chain growth process of $[Co(DAT)_6](ClO_4)_2$.

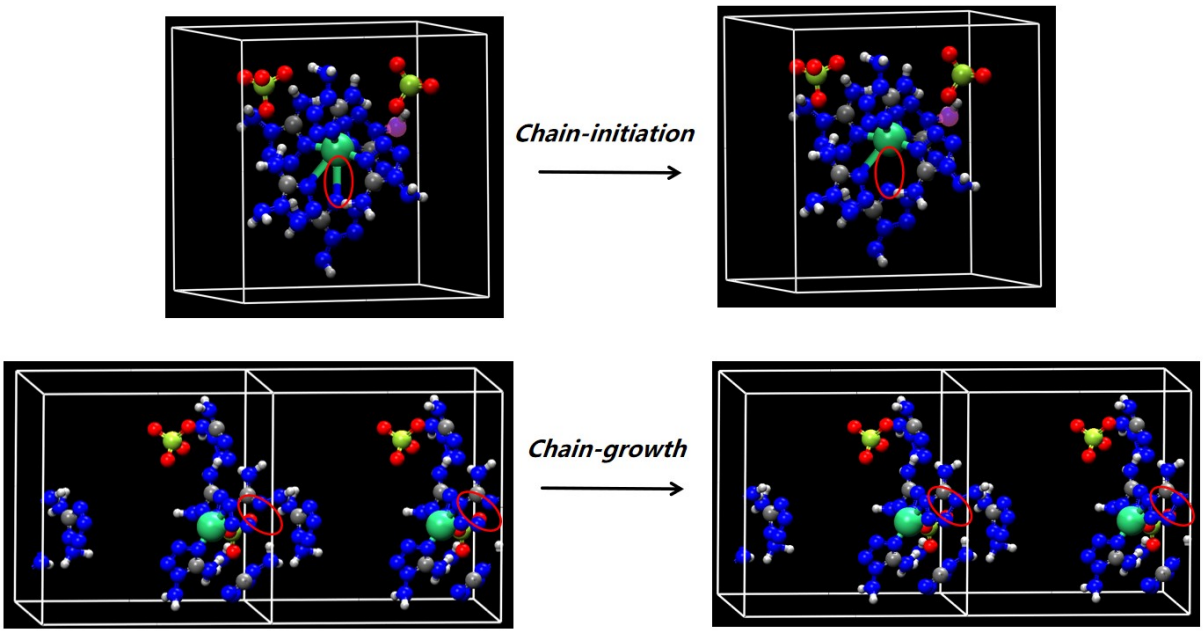

Figure S19. The snapshots of the chain initiation and chain growth process of $[Ni(DAT)_6](ClO_4)_2$.

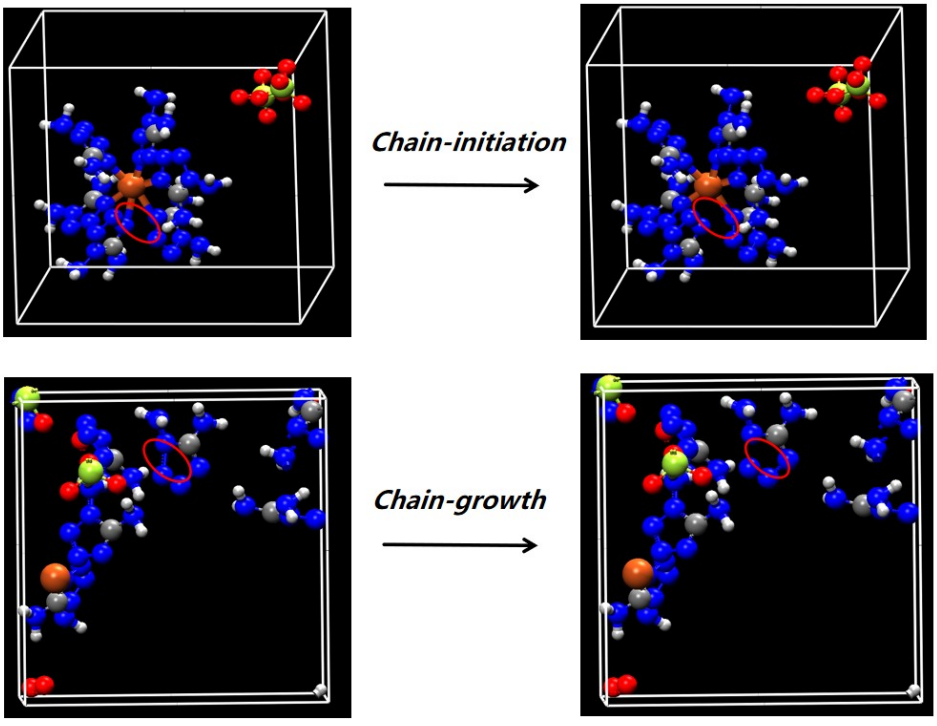

Figure S20. The snapshots of the chain initiation and chain growth process of $[Cu(DAT)_6](ClO_4)_2$.

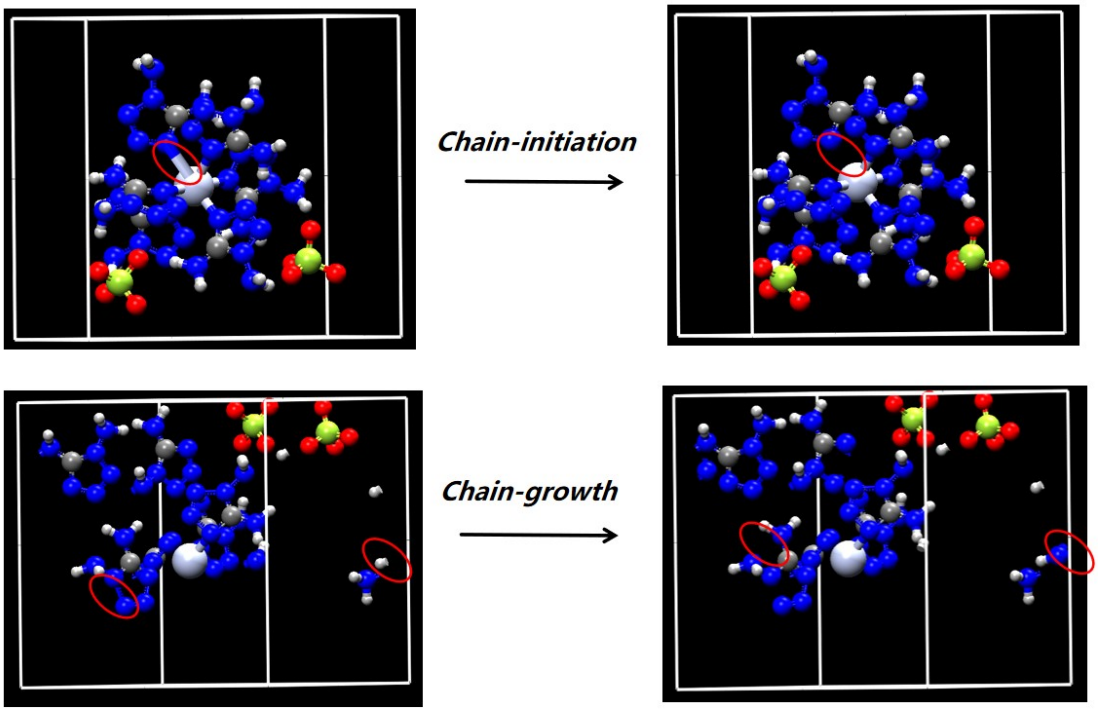

Figure S21. The snapshots of the chain initiation and chain growth process of $[Zn(DAT)_6](ClO_4)_2$.

Section 5 Optical characters

5.1 The effect of the ligands and anions

The peaks of NO_3^- and ClO_4^- are also similar with each other in the vis-NIR area. But for the electronic properties in Table 3, compare with 1-AT, DAT appears lower ionization energy (IE) and weaker electron affinity (EA). Therefore, DAT appears stronger Lewis basicity than that of 1-AT. ClO_4^- appears stronger IE and EA than that of NO_3^-.

Table S19 The ionization energy (IE) and electron affinity (EA) of center metal.

	DAT	ClO_4^-	1-AT	NO_3^-
EA	52.55	-230.01	-19.81	-182.85
IE	45.66	128.20	236.96	93.69

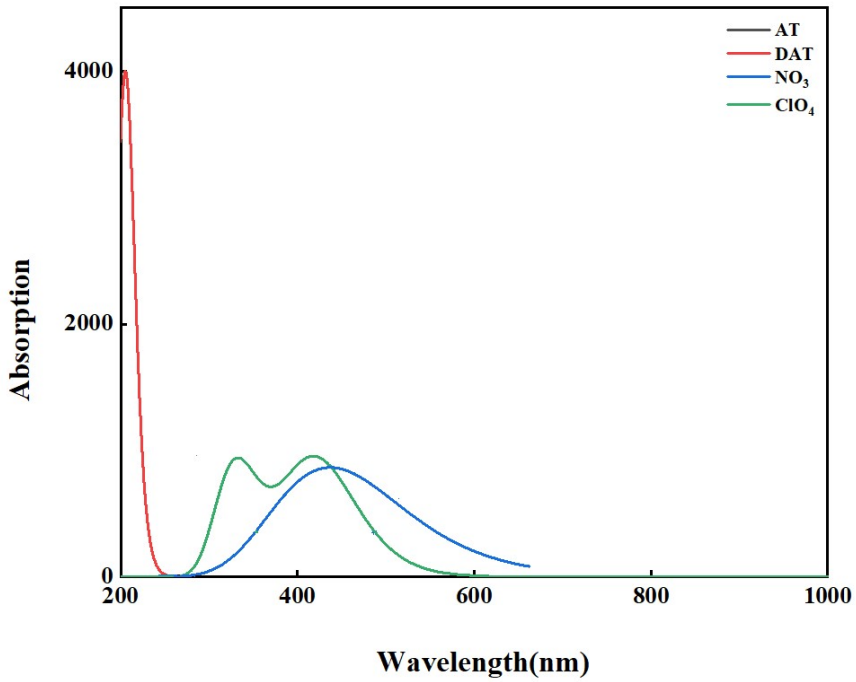

Figure S22 The absorption spectrum of 1-AT, DAT, NO_3^- and ClO_4^- ranged at 200 ~1000 nm.

5.2 The absorption characters of abstracted gas-phase molecules

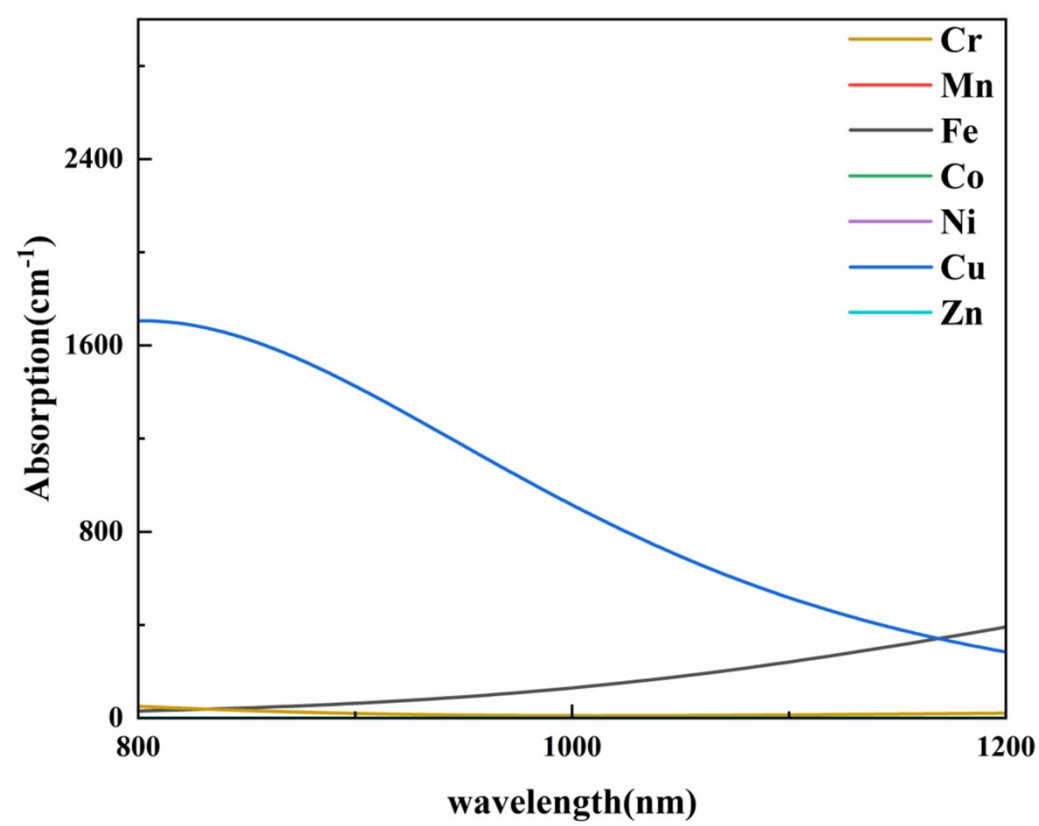

Figure S23 The absorption spectrum of seven Gas-phase bimoleculars ranged at 800 ~1200 nm.

5.3 Details of excited states and NIR excitation of molecules

Table S20 The excited states and NIR excitation (1.03~1.38 eV) with the corresponding energies, oscillator strengths and the CT modes of $[Cr(DAT)_6](ClO_4)_2$.

$[Cr(DAT)_6](ClO_4)_2$					
Excitation	**S0→S1**	**S0→S2**	**S0→S3**	**S0→S4**	**S0→S5**
Energy	0.0629 eV	0.1016 eV	0.1194 eV	0.1645 eV	0.3955 eV
(wavelength)	19726.81 nm	12198.66 nm	10380.67 nm	7538.40 nm	3134.51 nm
Oscillator strength	0.0035	0	0	0.02	0.021
Excitation	**S0→S6**	**S0→S7**	**S0→S8**	**S0→S9**	**S0→S10**
Energy(wave length)	0.5133 eV 241 5.64 nm	0.5551 eV 2233.49 nm	0.6162 eV 2012.20 nm	0.6626 eV 1871.24 nm	0.7372 eV 1681.92 nm
oscillator strength	0.013	0.045	0.067	0.004	0.037
Excitation	**S0→S14**	**S0→S15**	**S0→S20**		
Energy(wave length)	1.1642 eV 1065.01 nm	1.1675 eV 1061.95 nm	1.2582 eV		
oscillator strength	0.04	0.05	0.02		

Table S21 The excited states and NIR excitation (1.03~1.38 eV) with the corresponding energies, oscillator strengths and the CT modes of $[Mn(DAT)_6](ClO_4)_2$.

$[Mn(DAT)_6](ClO_4)_2$					
Excitation	**S0→S1**	**S0→S2**	**S0→S3**	**S0→S4**	**S0→S5**
Energy(wave length)	1.0072 eV 1230.99 nm	1.0315 eV 1202.00 nm	1.1339 eV 1093.43 nm	1.1581 eV 1070.55 nm	1.1782 eV 1052.30 nm
oscillator strength	0	0	0	0	0
Excitation	**S0→S6**	**S0→S7**	**S0→S8**	**S0→S9**	**S0→S10**
Energy(wave length)	1.1792 eV 1051.47 nm	1.2311 eV 1007.11 nm	1.2553 eV 987.71 nm	1.3052 eV 949.93 nm	1.3062 eV 949.23 nm
oscillator strength	0	0	0	0	0

Table S22 The excited states and NIR excitation (1.03~ 1.38 eV) with the corresponding energies, oscillator strengths and the CT modes of $[Fe(DAT)_6](ClO_4)_2$.

$[Fe(DAT)_6](ClO_4)_2$					
Excitation	**S0→S1**	**S0→S2**	**S0→S3**	**S0→S4**	**S0→S5**
Energy(wave length)	0.2697 eV 4597.05 nm	0.2738 eV 4528.97 nm	0.4832 eV 2565.77 nm	0.4967 eV 2496.06 nm	0.6437 eV 1926.03 nm
oscillator strength	0	0.001	0.002	0.002	0
	S0→S6	**S0→S7**	**S0→S8**	**S0→S9**	**S0→S10**
Energy(wave length)	0.7854 eV 1578.69 nm	0.7931 eV 1563.25 nm	0.9342 eV 1327.18 nm	1.0340 eV 1199.05 nm	1.0913 eV 1136.16 nm
oscillator strength	0	0.003	0	0.01	0.06
	S0→S11	**S0→S13**	**S0→S14**		
Energy(wave length)	1.2074 eV 1026.86 nm	1.2532 eV 989.46	1.4004 eV 885.33 nm		
oscillator strength	0.04	0.04	0.01		

Table S23 The excited states and NIR excitation (1.03~ 1.38 eV) with the corresponding energies, oscillator strengths and the CT modes of $[Co(DAT)_6](ClO_4)_2$.

$[Co(DAT)_6](ClO_4)_2$					
Excitation	**S0→S1**	**S0→S2**	**S0→S3**	**S0→S4**	**S0→S5**
Energy(wave length)	0.6371 eV 1946.20	0.6773 eV 1830.56 nm	0.8056 eV 1539.10 nm	0.9241 eV 1341.66 nm	0.9320 eV 1330.28 nm
oscillator strength	0	0	0	0	0
Excitation	**S0→S6**	**S0→S7**	**S0→S8**	**S0→S9**	**S0→S10**
Energy(wave length)	0.9644 eV 1285.60 nm	0.9726 eV 1274.79 nm	1.0485 eV 1182.45 nm	1.0930 eV 1134.34 nm	1.0934 eV 1133.93 nm
oscillator strength	0	0	0	0	0

Table S24 The excited states and NIR excitation (1.03~ 1.38 eV) with the corresponding energies, oscillator strengths and the CT modes of $[Ni(DAT)_6](ClO_4)_2$.

$[Ni(DAT)_6](ClO_4)_2$					
Excitation	**S0→S1**	**S0→S2**	**S0→S3**	**S0→S4**	**S0→S5**
Energy(wave length)	0.8921 eV 1389.74 nm	0.9174 eV 1351.45 nm	0.9326 eV 1329.49 nm	0.9578 eV 1294.48 nm	1.0389 eV 1193.44 nm
oscillator strength	0	0	0	0	0
Excitation	**S0→S6**	**S0→S7**	**S0→S8**	**S0→S9**	**S0→S10**
Energy(wave length)	1.0606 eV 1169.05 nm	1.0794 eV 1148.62 nm	1.0859 eV 1141.80 nm	1.0933 eV 1134.01 nm	1.1342 eV 1093.13 nm
oscillator strength	0	0	0	0	0

Table S25 The excited states and NIR excitation (1.03~ 1.38 eV) with the corresponding energies, oscillator strengths and the CT modes of $[Cu(DAT)_6](ClO_4)_2$.

$[Cu(DAT)_6](ClO_4)_2$					
Excitation	**S0→S1**	**S0→S2**	**S0→S3**	**S0→S4**	**S0→S5**
Energy(wave length)	0.1860 eV 6667.08 nm	0.2462 eV 5035.25 nm	0.3838 eV 3230.39 nm	0.4622 eV 2682.65 nm	0.6531 eV 1898.49 nm
oscillator strength	0.0042	0.0160	0.024	0.068	0.04
Excitation	**S0→S6**	**S0→S7**	**S0→S8**	**S0→S9**	**S0→S10**
Energy(wave length)	0.7015 eV 1767.38 nm	0.8602 eV 1441.34 nm	1.1260 eV 1101.13 nm	1.4571 eV 850.92 nm	1.5277 eV 811.60 nm
oscillator strength	0.04	0.11	0.16	0.007	0.024

Table S26 The excited states and NIR excitation (1.03~ 1.38 eV) with the corresponding energies, oscillator strengths and the CT modes of $[Zn(DAT)_6](ClO_4)_2$.

$[Zn(DAT)_6](ClO_4)_2$					
Excitation	**S0→S1**	**S0→S2**	**S0→S3**	**S0→S4**	**S0→S5**
Energy(wave length)	0.8894 eV 1393.95 nm	0.9289 eV 1334.76 nm	1.0539 eV 1176.43 nm	1.0610 eV 1168.51 nm	1.0939 eV 1133.41 nm
oscillator strength	0	0	0	0	0
Excitation	**S0→S6**	**S0→S7**	**S0→S8**	**S0→S9**	**S0→S10**
Energy(wave length)	1.2264 eV 1010.93 nm	1.2966 eV 956.25 nm	1.3858 eV 894.70 nm	1.4613 eV 848.48 nm	1.5045 eV 824.11 nm
oscillator strength	0	0	0	0	0

5.4 Proportions of holes and electrons in charge transition of $[Cr/Fe/Cu(DAT)_6](ClO_4)_2$

Table S27 Proportions of holes and electrons of $[Cr(DAT)_6](ClO_4)_2$ in charge transition.

$[Cr(DAT)_6](ClO_4)_2$	S14		S15		S20	
	Hole	**Electron**	**Hole**	**Electron**	**Hole**	**Electron**
M^{2+}	73.43 %	1.47 %	0.07 %	0.00 %	72.85 %	1.44 %
Ligands	26.50%	97.51%	2.53%	0.01 %	19.81%	98.51%
ClO_4^-	0.03%	0.01%	0.00 %	0.00 %	0.03%	0.01%
M^{2+}	0.01 %	0.19 %	68.48 %	1.73 %	0.55 %	0.01 %
Ligands	0.02 %	0.83%	28.89%	98.24%	0.79%	0.01 %
ClO_4^-	0.00 %	0.00 %	0.04%	0.01 %	0.00 %	0.04%

Table S28 Proportions of holes and electrons of $[Fe(DAT)_6](ClO_4)_2$ in charge transition.

$[Fe(DAT)_6](ClO_4)_2$	S9		S10		S11		S13	
	Hole	**Electron**	**Hole**	**Electron**	**Hole**	**Electron**	**Hole**	**Electron**
M^{2+}	0.01 %	0.65 %	0.01 %	11.18 %	0.01 %	0.18 %	0.01 %	0.18 %
Ligands	1.79%	99.28	1.73%	88.17%	1.74%	1.71%	1.80%	2.38%
ClO_4^-	48.50%	0.03%	46.69%	0.11%	46.72%	1.42 %	48.29 %	4.13 %
M^{2+}	0.44 %	0.00 %	1.39 %	0.05 %	1.36 %	11.21 %	0.56 %	4.30%
Ligands	49.11%	0.03 %	50.02%	0.48%	50.00%	85.44%	49.20%	89.11%
ClO_4^-	0.14 %	0.00 %	0.14 %	0.00 %	0.14 %	0.03%	0.15 %	0.03 %

Table S29 Proportions of holes and electrons of $[Cu(DAT)_6](ClO_4)_2$ in charge transition.

$[Cu(DAT)_6](ClO_4)_2$	S8	
	Hole	**Electron**
M^{2+}	12.05 %	0.93 %
Ligands	34.07%	41.04%
ClO_4^-	0.04%	0.19 %
M^{2+}	20.51 %	0.08 %
Ligands	8.02%	9.86%
ClO_4^-	25.31 %	47.91 %